Fully-Implicit Relational Coarsest Partitioning for Faster Bisimulation (As Preparation for Fully-Implicit Lumping)

Malcolm Mumme

September 24, 2008

1 Abstract

The present work applies interleaved MDD partition representation to the bisimulation problem. In the course of considering fully-implicit lumping (see section 2.6) for Markov systems, we have implemented fully-implicit partitioning, using interleaved MDDs for bisimulation partitioning, in the context of the SMART verification tool. We compare the execution time and memory consumption of our fully-implicit methods (using interleaved MDDs) with the execution time and memory consumption of partially-implicit methods (using non-interleaved MDDs), as applied to the same bisimulation problems. We found that the fully implicit method had prohibitively large run-times for models with few variables with many values. The performance of the fully implicit method was reasonable for models with many variables having few values, although generally slower than the hybrid method which used non-interleaved MDDs to represent the state-space partition.

2 Introduction

The formal verification of properties of moderately complex systems frequently involves operations on finite-state automata (FSA) that are very large (containing many states). Algorithms for verification of system properties can require time that grows much worse than linearly in the size of the relevant FSA. The *bisimulation* operation involves (hopefully implicit) comparison of all FSA states to determine if they are (extensionally) distinguishable. The FSA are frequently so large, that they must be stored using a *symbolic* representation, which itself may be quite large. As such large FSA have prohibitive resource requirements, additional improvements are desired. Fortunately, properties of FSA that need to be verified are usually defined extensionally. The results of verification depend only on the behavior of the input FSA, and not intensional characteristics, such as the details of their representation. Conveniently, the input FSA are often not the smallest FSA having the same behavior. Consequently, one may often replace the input FSA with equivalent smaller FSA having the same behavior, using the largest bisimulation to find the smallest equivalent FSA. The search for the largest bisimulation of a given FSA is called the *relational coarsest partitioning* problem. The *lumping* problem (which motivates the present work) is an analogous problem pertaining to the solution of Markov systems, described later. The relational coarsest partitioning problem was solved optimally (for explicit representations) by Paige and Tarjan [14] in 1987. Other solutions ([1] [8] [19] discussed below) to this problem have been found for FSA in symbolic representations. We expected the current work to represent an improvement on these methods.

2.1 SMART

SMART (Stochastic Model checking Analyzer for Reliability and Timing) (see `http://www.cs.ucr.edu/~ciardo/SMART`) is a modeling and verification tool that implements various forms of model checking and Markov system analysis, among other things. When so directed, SMART applies symbolic methods to the solution of model checking problems and the solution of Markov systems. As research in these areas progresses, improved methods of solution are integrated with the SMART tool. The present work implements one of these steps in the evolution of SMART.

2.2 *Symbolic* Methods

Symbolic methods in model checking are distinct from the more commonly known *mathematical* symbolic methods. Mathematical symbolic methods employ finite symbolic formulas to represent a much larger (usually countably infinite) collection of facts. For example, the finite formula: $\forall x, y \in \mathbb{N} : x + y = y + x$ represents an infinitely large number of simple facts: $0 + 0 = 0 + 0$, $0 + 1 = 1 + 0$, $1 + 0 = 0 + 1$, $1 + 1 = 1 + 1$, $0 + 2 = 2 + 0$, $1 + 2 = 2 + 1$, $2 + 0 = 0 + 2$, $2 + 1 = 1 + 2$, $2 + 2 = 2 + 2$, etc.

By contrast, symbolic methods in model checking employ finite data structures to represent other (usually much larger) finite collections of data. Figure 1, for example, contains 2 different pictures of a symbolic representation for the bit string "1000011101111100".

Typically, *Decision Diagrams (DDs)* are the finite data structures employed, and they represent finite sets, relations, and functions. The following types of decision diagrams are explained individually in the following subsubsections. *(Ordered) Binary Decision Diagrams ((O)BDDs)* typically are used to represent sets of states of systems where each component of a state is binary, such as the states of bits in a register. BDDs can also represent relations between sets of such states. *Multi-way Decision Diagrams (MDDs)* typically are similarly used on such systems except where each component of a state has some finite number of values (possibly greater than 2), such as certain Petri nets. *Multi-Terminal Decision Diagrams (MTDDs)* can represent mappings from states (of various kinds) onto any explicitly represented finite set. *Edge-Valued Binary Decision Diagrams (EVBDDs)* can compactly represent functions from states (with binary components) onto reals (floats, actually). *Edge-Valued Multi-way Decision Diagrams (EVMDDs)* can similarly represent functions from states (with multi-valued components) onto reals. *Affine Algebraic Decision Diagrams (AADDs)* can be used similarly to EVDDs, and support some combinations of operations more efficiently.

The various kinds of decision diagrams support efficient algorithms for a variety of operations. OBDDs and MDDs provide support for efficient set operations, such as union, intersection, and difference. When used to represent relations, they also support composition, application, and transitive closure, with somewhat more effort. MTDDs support efficient arbitrary pairwise operations on the represented functions (that is, computing $H \leftarrow F \odot G$, so that $H(x) = F(x) \odot G(x)$, for arbitrary operations $\odot$), and efficient reduction operations, provided that the ranges of all functions remain of reasonable (small) size. Some EVDDs (EV+DDs) efficiently support pairwise addition and subtraction, as well as summation operations, while others (EV*DDs) efficiently support pairwise multiplication and division, as well as product operations. AADDs efficiently support pairwise addition, subtraction, multiplication, division, minimum and maximum, as well as summation and product operations.

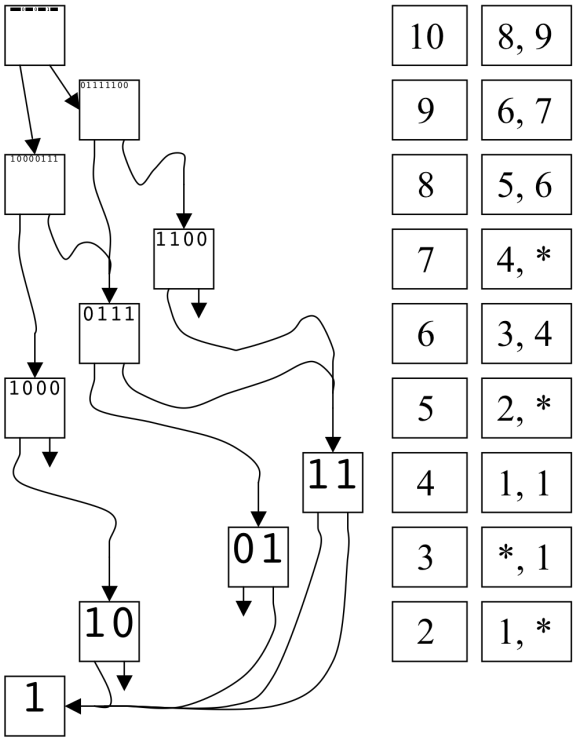

Figure 1: A symbolic representation for a sequence of bits (1000011101111100). Here, each node is labeled with a sequence of bits, which is represented by the subtree starting at that node. Each subtree, starting at some node, represents the sequence of bits constructed by concatenating the sequences of bits represented by the subtrees starting at the children of that node. In this binary diagram, notice that each node has a bit string twice as long as those of its children. Arrows going nowhere point to imaginary nodes containing an appropriate number of zeros. The table on the left shows how this tree might be represented in the memory of a computer. Each row corresponds to a node in the diagram, and the two numbers in the rightmost box of each row indicate destinations of arrows from the corresponding node. "*"s represent arrows going nowhere.

2.2.1 (Ordered) Binary Decision Diagrams (BDDs) [2]

BDDs use a binary tree-like structure to represent a (hopefully larger) table of booleans, or anything representable as a table of booleans. A set of binary register states can be mapped to a table of booleans, by constructing the table index from the bits of the state. Consider the domain $[0, 15]$, which could represent the 16 states { "0000", ... "1111" } of a 4-bit register. We show how to represent a subset $\{0, 5, 6, 7, 9, 10, 11, 12, 13\}$ = { "0000" , "0101" , "0110" , "0111" , "1001" , "1010" , "1011" , "1100" , "1101" } of this domain as a table of booleans. In one column, list the domain elements in order. In the second column, enter "0" in those rows ($\{1, 2, 3, 4, 8, 14, 15\}$) where the domain element is not in the set, and enter "1" in those rows ($\{0, 5, 6, 7, 9, 10, 11, 12, 13\}$) where the domain element is in the set.

0 “0000”	1
1 “0001”	0
2 “0010”	0
3 “0011”	0
4 “0100”	0
5 “0101”	1
6 “0110”	1
7 “0111”	1
8 “1000”	0
9 “1001”	1
10 “1010”	1
11 “1011”	1
12 “1100”	1
13 “1101”	1
14 “1110”	0
15 “1111”	0

The contents of the second column comprise a bit string “1000011101111100” (or table of booleans) that represents the subset $\{0, 5, 6, 7, 9, 10, 11, 12, 13\}$. Next, we will illustrate the transformation of the table of booleans into a corresponding BDD. Figure 2 (left) shows an *unreduced* binary tree representing the same bit string. In the bottom row are leaves of the tree, that are considered to represent individual 1's and 0's. In the other rows are nodes, each with two ordered outgoing edges. So that the correctness of this representation will be conspicuous, each of these nodes is labeled with a bit string it is considered to represent, and the nodes are drawn with sizes proportional to the sizes of the bit strings they represent. Note that at each level of the tree, all the bit string sizes are the same, being half the size of the bit strings represented by nodes of the preceding level. Also note that edges from a level only target nodes at the very next level.

Except for the leaves, each level of the tree is associated with a single one of the four bits in the state of the register being modeled. The top, or root, node of the tree is associated with the leftmost register bit, while the lowest (other than the leaves) is associated with the rightmost register bit. Each outgoing edge from a node is associated with a specific value of the bit associated with the node's level. The leftmost edge is associated with the value 0, while the rightmost edge is associated with the value 1. These associations provide the following simple method, using the binary tree, for testing if a specific register state is a member of the represented set. Starting at the root of the tree, consider consecutive bits of the register state. For a bit whose value is 0, move down the left edge from the node, and consider the next bit of the state. Likewise, if a bit has the value 1, move down the right edge from the node, and consider the next bit of the state. Proceeding thusly, until the bits of the state are exhausted, a leaf node is found. The state is a member of the represented set iff the leaf has the label “1”. This procedure, together with the BDD contents, can be thought of as an implementation of the characteristic function of the set, and, at the same time, as an implementation of the constant table of booleans from which it was derived.

As examples, consider the states 6 (“0110”), and 14 (“1110”). To test state 6 for membership, start at the root, and consider the first bit (“0”) of state 6. Selecting the left edge leads to the node labeled “10000111”, then consider the second bit (“1”) of state 6. Select the right edge to find the node labeled “0111”, and proceed to the third bit, also “1”. Follow the right edge to the node labeled “11”, and consider, finally the last bit of state

6, a "0". The left edge targets a leaf node labeled "1"; consequently we know that state 6 is a member of the set. With state 14, we start again at the root, and according to the values of the consecutive bits ("1", "1", "1", and "0"), we select the right edge, proceeding to the "01111100" node, the right edge of that, going to the node marked "1100", the right edge of that node, targeting a "00" node, then the left edge of that, ending in a leaf node marked "0", showing that state 14 is not a member of the represented set.

Figure 2 (middle) shows a related graph, after partial *reduction*. The difference between this graph and the graph in Figure 2 (left) is the removal of redundant nodes. Each node representing the same value, as some node to its left, has been removed. Edges targeting removed nodes have been adjusted to target remaining nodes representing the same value. Although this example shows a very minor decrease in size due to reduction, BDDs representing FSMs in model checking applications frequently exhibit a size improvement by many orders of magnitude, between the *quasi-reduced* BDD and the corresponding unreduced BDD.

Figure 2 (right) simply shows the same graph, where the nodes are drawn with constant size. An additional small

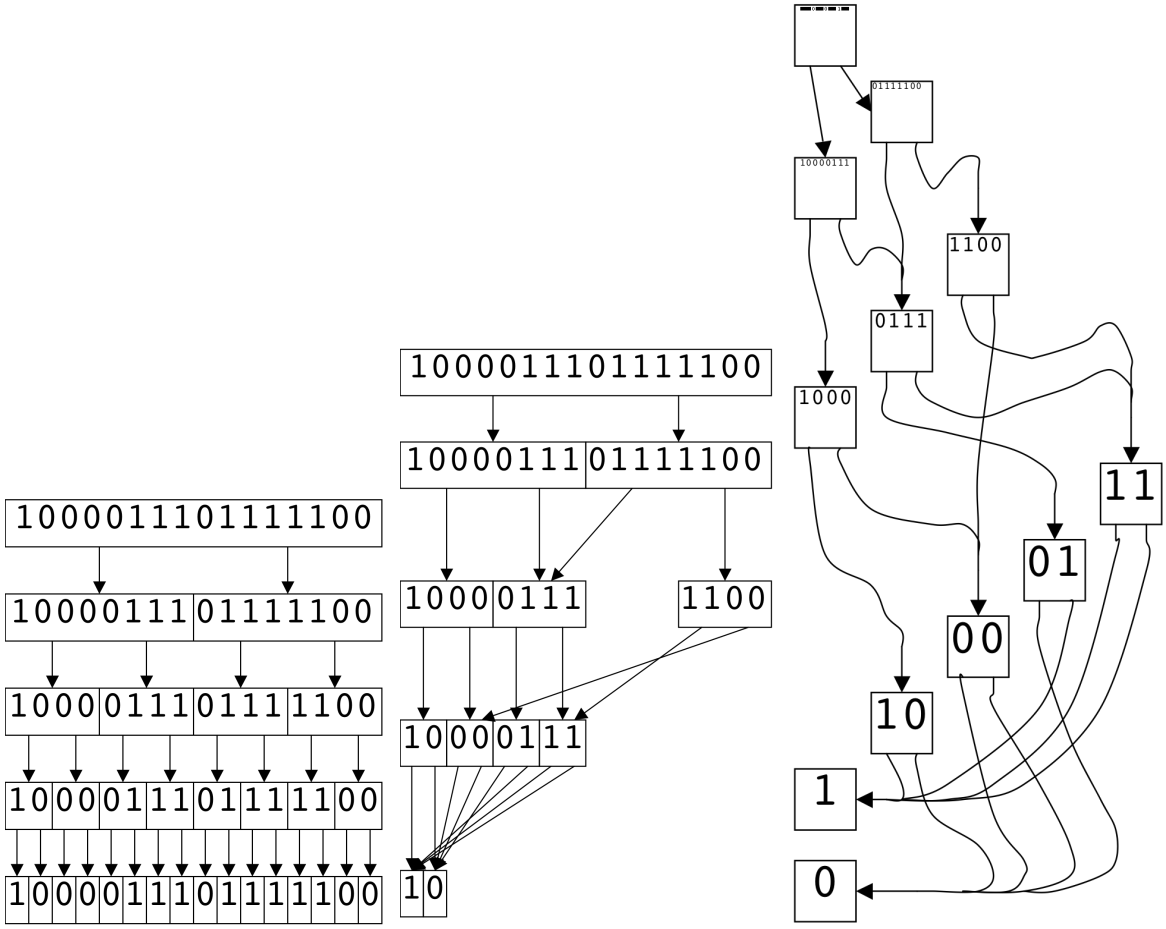

Figure 2: Binary trees for "1000011101111100".

improvement can be obtained by removing nodes which represent bit strings containing only "0"s. Edges targeting such nodes are replaced by special *NULL* edges, here drawn as arrows leading nowhere. The result is the BDD previously shown as Figure 1 (left). As long we know that the size of the string represented at each level, we can easily determine the number of "0"s represented by a given NULL edge, since it previously targeted a node representing a bit string that was half the size of the bit strings represented at the previous level. The above method for membership testing still applies to partially reduced graphs, except that upon encountering a NULL edge, one may immediately conclude that the element is not a member of the set. Figure 1 (right) illustrates a

possible tabular computer representation of the graph in Figure 1 (left).

It is still possible to decrease the size of the graph by removing nodes where all outgoing edges target the same node. Any edges targeting such a node are retargeted to the targets of edges of the removed node. In such a *fully reduced* representation, it is necessary to mark each node with an indication of its level, since edges are no longer limited to proceed from one level to the very next level.

Fully reduced diagrams are sometimes preferred for reasons of storage efficiency; however, they will not be discussed further here, as they would complicate the explanation of relevant algorithms. The above method for membership testing, for example, must be modified to use the level markings to determine which state bit to consider. Additional variations and extensions of BDDs are used, some of which are described later.

2.2.2 (Ordered) Multi-way Decision Diagrams (MDDs) [11]

Whereas nodes of quasi-reduced BDDs always have two outgoing edges, MDDs have no such restriction, but are otherwise similar. They occur in unreduced, quasi-reduced and fully reduced varieties, and with additional extensions yet to be described. MDDs are ideal for storing a set of states of a machine where the individual state variables that compose the state have more that two different values. As with BDDs, reduced and quasi-reduced varieties of MDDs provide multiple orders of magnitude improvement in the size of representations used in many model checking problems.

Consider a state machine with four individual variables, whose values are in the domain $\{0, 1, 2\}$. We could use a notation such as "0221" to denote the state where the first variable has the value "0", the second and third variables have the value "2", and the fourth and last variable has the value "1". Figure 3 shows an MDD representation of a set of states { "0001", "0010", "0100", "0111", "1011", "1020", "1110", "1121", "2000", "2021", "2101", "2120" } of this machine.

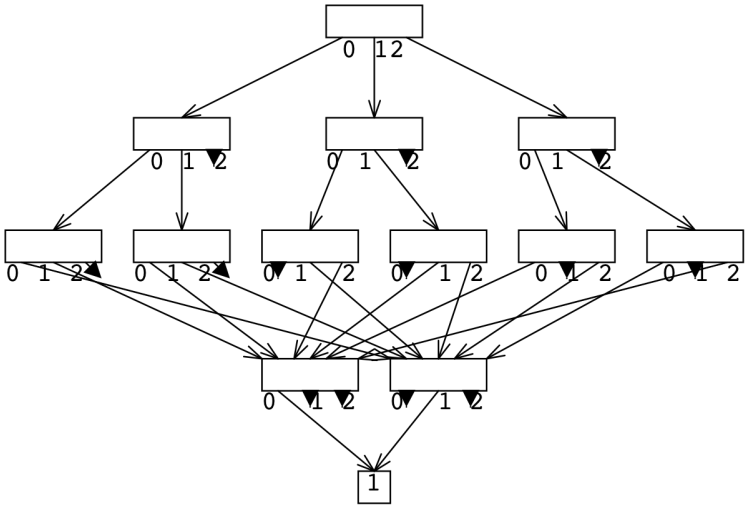

Figure 3: MDD{"0001", "0010", "0100", "0111", "1011", "1020", "1110", "1121", "2000", "2021", "2101", "2120"}.

In this diagram, the edges are labeled with associated values, while the nodes have not been labeled. This graph is quasi-reduced. The full tree, even if NULL edges were used, would require ten additional non-leaf nodes, and

eleven redundant leaf nodes labeled "1". A slightly modified method for testing membership may be used with this form of decision diagram. As with BDDs, start at the root node, and consider consecutive variables. Follow the edge from the current node whose label matches the value of the variable, then consider the next variable. If a NULL edge is followed, or the leaf node "0" is found, the element is not in the represented set, while arrival at the leaf node "1" indicates membership in the set.

This diagram, derived from a simple model, can also illustrate the importance of *variable ordering*. It has been found that careful choice, of the order in which to consider variables, can be used to significantly decrease the size of decision diagrams. We illustrate this by exchanging positions of the second and third variable, and constructing a new quasi-reduced diagram from the resulting table.

We start with a table of states, in lexicographic order:

The ordered state table:

"0001"
"0010"
"0100"
"0111"
"1011"
"1020"
"1110"
"1121"
"2000"
"2021"
"2101"
"2120"

, then exchange positions:

"0001"
"0100"
"0010"
"0111"
"1101"
"1200"
"1110"
"1211"
"2000"
"2201"
"2011"
"2210"

, then reorder the table:

"0001"
"0010"
"0100"
"0111"
"1101"
"1110"
"1200"
"1211"
"2000"
"2011"
"2201"
"2210"

.

Then produce the new diagram from the (lexicographically) reordered table. The resulting diagram, pictured in Figure 4, has one third fewer non-leaf nodes than the previous diagram. As with many other optimizations, careful variable ordering can produce orders of magnitude reduction in the size of many large diagrams. In the general case, determination of the optimal variable ordering, to reduce MDD size, is a difficult problem. Fortunately, effective heuristics have been found for variable order choice, that produce very good reductions in MDD size. These heuristics are vaguely based on the notion that related variables should be placed near each other in the ordering. In the above example, in Figure 3, the first and third variables were related to each other in the original problem, as were also the second and fourth variables. In the reordered MDD, in Figure 4, where the second and third variables were switched, the related variables became adjacent, resulting in the improvement in BDD size. We shall see later exactly how those variables were related.

Although the MDDs shown so far have each had a fixed number of edges associated with the non-leaf nodes, there is no requirement for an MDD to do so. In fact, there are important algorithms which depend on the use of MDDs where the number of edges is not fixed, and cannot even be determined a priori.

2.2.3 Multi-Terminal Decision Diagrams (MTDDs) [9]

In the same way that BDDs and MDDs are equivalent to tables of booleans, MTDDs are equivalent to tables of values from any finite type. That is, they implement functions with arbitrary finite ranges, as opposed to

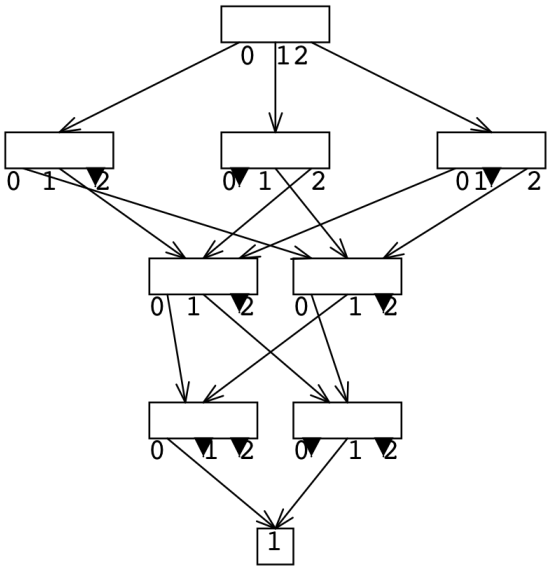

Figure 4: MDD for {“0001”, “0010”, “0100”, “0111”, “1011”, “1020”, “1110”, “1121”, “2000”, “2021”, “2101”, “2120”}, after reordering (switching second and third variables) to: {“0001”, “0100”, “0010”, “0111”, “1101”, “1200”, “1110”, “1211”, “2000”, “2201”, “2011”, “2210”}.

characteristic functions (with boolean range). MTDDs can also be a BDD (MTBDD) or an MDD (MTMDD), the main difference being that plain BDDs and MDDs have leaf nodes with values “0” and “1”, while MTDDs can have values from the associated finite type. As an illustration of MTDDs, an MTMDD for the “Rock-Paper-Scissors” game is shown in Figure 5. The range of the function is { win, loose, draw }. The diagram shows the outcome of the game, for player 1, given that the first variable represents the choice made by player 1, and the second variable represents the choice made by player 2. The procedure for evaluating a function, represented this way, is

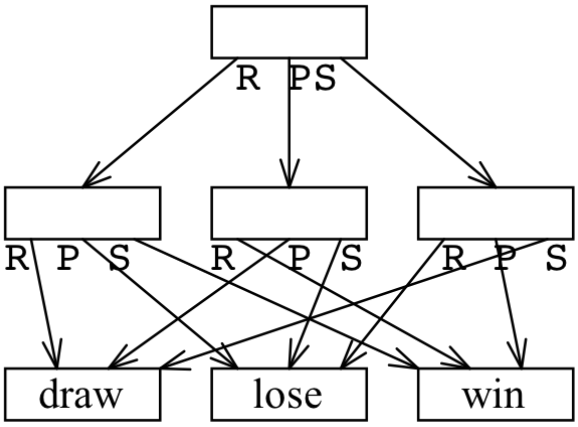

Figure 5: MTMDD for “Rock-Paper-Scissors” game.

similar to the membership testing procedure for MDDs. The leaf node one arrives at, at the end of the procedure, determines the value of the function.

It should be noted that, although the range of such functions would usually be drawn from simple enumerable types, the range could also be a finite subset of some continuous set, such as the reals. If a bet was riding on the outcome of the game, for example, then the range of the function might be { 0.0, -5.0¢, +5.0¢}.

Some algorithms [5] for Markovian Lumping use this type of MTDD to represent functions onto $\mathbb{R}$, by adjusting the range to match the finite set of values of interest at a particular time. Note that this use of MTDDs is *explicit* in the number of different values in the range of the function. That is, a separate component of the data structure must exist for each distinct value in the range. Consequently, the size of an MTDD representing some function f, is at least O($|range(\ f\ )|$).

2.2.4 Edge-Valued Multi-way, and Binary, Decision Diagrams (EVMDDs, EVBDDs) [12]

EVDDs can represent functions, onto a finite subset of $\mathbb{R}$, in a way that is not explicit in the size of the domain. This can be done by associating a real function with each edge.

The general method for evaluating functions represented this way is as follows: Retain a current value, whose initial value depends on the type of EVMDD. Sometimes there is a special start edge, which must be followed to arrive at the root node. Start by following the start edge to the root node, and consider the values of the domain variables consecutively, following the edge selected according to the value of the domain variable. While following an edge, apply the associated real function to the retained current value. Eventually one arrives at the sole leaf node, (usually labeled Ω). The current value, at that time, is the value of the function.

Several different styles of EVDD exist, three of which are illustrated by examples below.

1. (Additive) Edge-Valued Decision Diagrams (EV^+MDDs) [3] [12]

   EV^+MDDs are most convenient for functions that range over values which are each the sum of some subset of a given small finite subset of $\mathbb{R}$. The function, associated with an edge of an EV^+MDD, adds a constant, called the weight, to the input, to produce the output. EV^+MDDs will be drawn here showing the weights associated with the edges. Consider the rock-paper-scissors game, repeated 4 times, where 5¢, 10¢, 15¢, and 20¢, are bet on each consecutive game. The cumulative outcome, for one of the players, of these games, can be calculated as the sum of some subset of $\{-20, -15, -10, -5, 5, 10, 15, 20\}$. An EV^+MDD representing this function of the players choices is shown in Figure 6 (left). With EV^+MDDs, the current value is typically initialized to 0.0.

   The desire to use reduced DDs brings about the need to enforce *canonicity*. Consider the two EV^+MDDs in Figure 7. It should be discernible, from inspection, that both EV^+MDDs represent the same function. Suppose that these DDs are actually sub-trees of a larger EV^+MDD. As they represent the same function, we would like for these trees to become a single tree, in a reduced EV^+MDD. However, as the trees are not identical, it is not very obvious that they represent the same function.

   To avoid this situation, we apply a *normalization condition* to trees, to make them *canonical*. Some systems, such as SMART, normalize EV^+MDDs so that they have no negative weights, except for the starting edge, as required by the normalization condition. The normalization condition additionally requires that at least one outgoing edge, from any node with an outgoing edge, will have a weight of 0. These normalization requirements make subtrees canonical, so that subtrees representing the same function will be identical. The EV^+MDD, on the right side of Figure 7, has been normalized with this condition. One can also consider the EV^+MDD, on the left side of Figure 7, to be normalized with an alternate condition, that requires the values represented by a subtree to have a mean value of 0, ignoring the incoming "start" edge. With these things in mind, one can now see, from inspection, that the two EV^+MDDs in Figure 6 both represent the same function. The EV^+MDD on the left is normalized with the 0-mean condition, while the one on the right is normalized with the non-negative condition. To fully benefit from reduction, of course, all subtrees

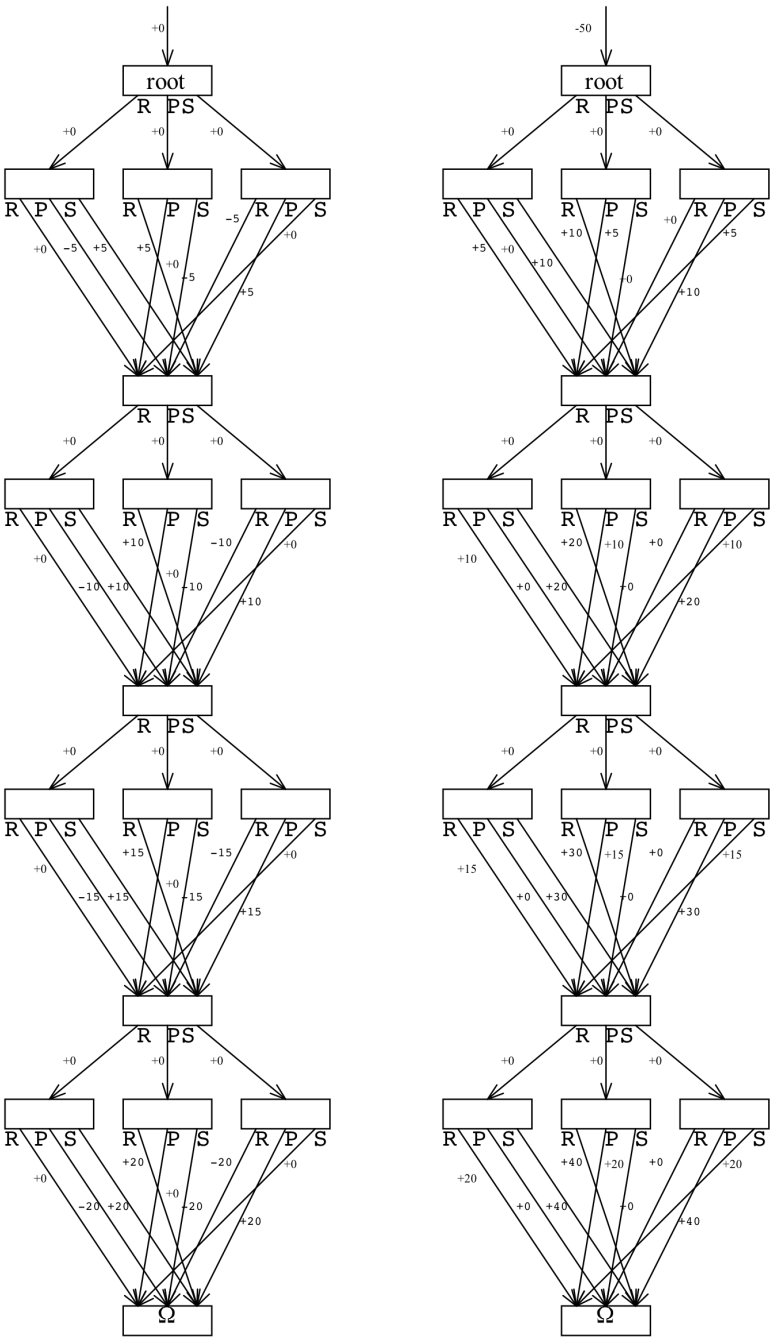

Figure 6: EV$^+$MDDs for payoff function for a series of 4 "Rock-Paper-Scissors" games.

of a tree should follow a common normalization condition. Different normalization conditions have special benefits in different circumstances. EV$^+$MDDs normalized with the non-negative condition have advantages in certain applications [3] involving extended natural numbers (where the range is $\mathbb{N} \cup \{\infty\}$).

2. (Multiplicative) Edge-Valued Decision Diagrams (EV*MDDs) [18]

   Similarly to EV$^+$MDDs, EV*MDDs are convenient for representing functions that range over values which are each the product of some subset of a given small finite subset of $\mathbb{R}$. Such functions occur in applications such as stochastic lumping, where the transition rates of a set of state transitions may be represented as EV*MDDs. The edge-associated function of an EV*MDD multiplies a constant weight with the input, to produce the output. Any EV$^+$MDD can be transformed, into an EV*MDD, by replacing the initial value and each weight with the exponential function of the corresponding weight. Although such a transformation may

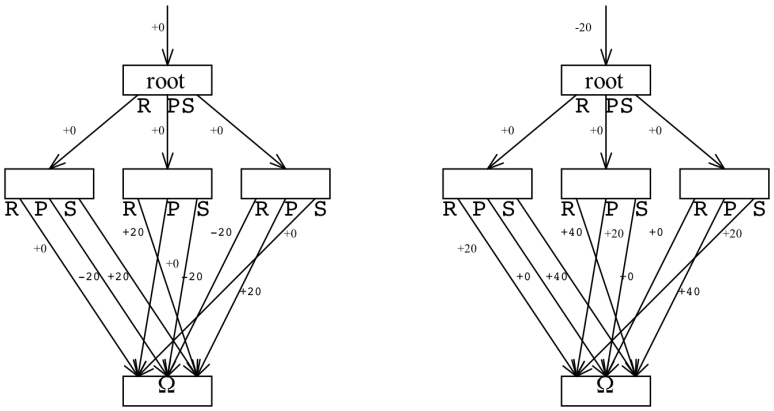

Figure 7: EV$^+$MDDs for payoff function for "Rock-Paper-Scissors" game.

have no practical meaning to an application, its existence shows that normalization conditions that apply to EV$^+$MDDs may be transformed to normalization conditions that apply to EV*MDDs. Corresponding to the 0-mean normalization condition for EV$^+$MDDs, a possible normalization condition for EV*MDDs is one that requires the geometric mean of values represented in a subtree to always be 1.0. The non-negative normalization condition for EV$^+$MDDs would correspond to a condition, for EV*MDDs, where the edge weights are required to have magnitudes of at least 1.0, except for the start edge.

As an illustration, consider the above-mentioned series of Rock-Paper-Scissors games. If we know a-priori the probability of the player's choices are independent of history, and the values of the probabilities, we can produce an EV*MDD that efficiently encodes the probability of any given sequence of choices. The EV*MDD, shown in Figure 8, does so, given that the players make choices with probability given in the following table:

	Rock	Paper	Scissors
player 1	60%	20%	20%
player 2	30%	30%	40%

3. Affine Algebraic Decision Diagrams (AADDs) [15] (similar to FEVBDDs) [17]

   AADDs combine most of the benefits of both EV+DDs and EV*DDs. It has been shown [15] that, for some functions, AADDs can provide an exponential improvement in the size of the representation, as compared to BDDs. The edge function is affine, evaluated by multiplication with a constant weight, and addition of another constant offset. Both constants are stored associated with the edge. AADDs are can be normalized in such a way that all range values are in $(0, 1]$, so they may be ideal for functions that yield probability values, such as those which occur in analysis of stochastic Markov chains.

2.3 Representation of sets, relations and functions using Decision Diagrams

Use of the appropriate form of decision diagram for the representation of sets, relations, and functions can provide multiple orders of magnitude improvement in the size of the representations, as well as in the computation time required for operations on those objects, as compared with the use of explicit representations.

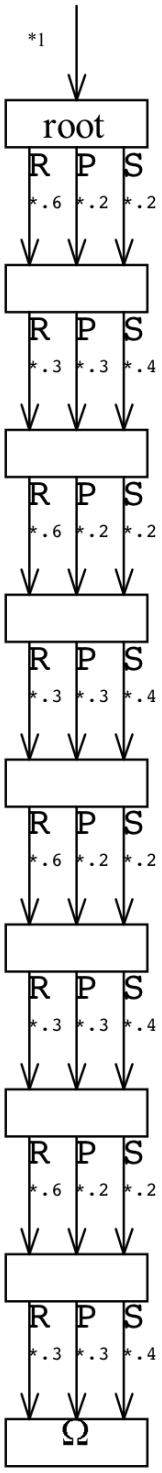

Figure 8: (non-normalized) EV*MDD for probability of a series of 4 "Rock-Paper-Scissors" games.

2.3.1 Representation of sets using Decision Diagrams

In decision diagrams, sets are represented implicitly. That is, sets are represented as a graph, which was reduced from a tree, which was derived from a boolean table of all values of the characteristic function of the represented set. Thus sets are represented as boolean functions, converted to tables, then trees, then reduced to decision diagrams. Hence, if one wished to represent a multi-set, one might start by converting its characteristic function to a table of integers, then to a tree, then reducing it to a MTDD or to an EVDD.

2.3.2 Representation of relations using Decision Diagrams

Relations may be represented as sets, by considering them to be sets of pairs, or other tuples, as one is likely to do in a study of relational algebra. One way to obtain a representation of the value of a tuple is to concatenate the values of the variables belonging to all the elements of the tuple. Another way to represent the value of a tuple will be discussed in section 2.3.3. Converting all such representations, that apply to a particular relation, to a table of booleans provides the necessary characteristic function for building a decision diagram.

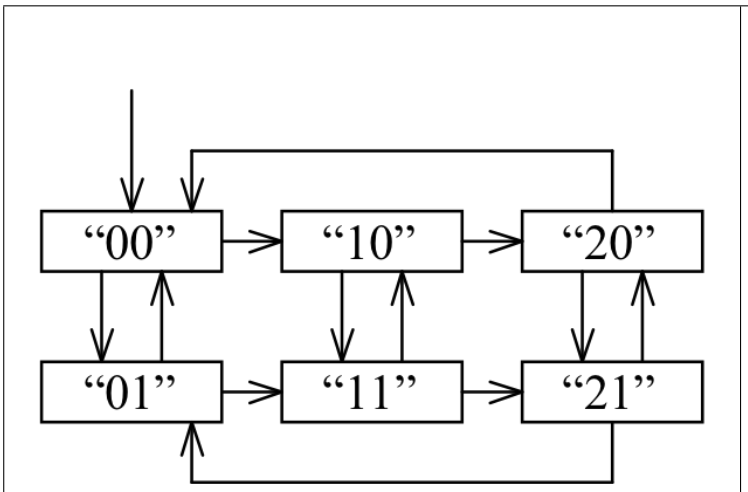

⟨ “00” → “01” ⟩
⟨ “00” → “10” ⟩
⟨ “01” → “00” ⟩
⟨ “01” → “11” ⟩
⟨ “10” → “11” ⟩
⟨ “10” → “20” ⟩
⟨ “11” → “10” ⟩
⟨ “11” → “21” ⟩
⟨ “20” → “00” ⟩
⟨ “20” → “21” ⟩
⟨ “21” → “01” ⟩
⟨ “21” → “20” ⟩

Figure 9: A FSA and its transition relation (without edge labels).

Consider the state transition relation for the FSA shown in Figure 9 (left). The FSA shown in Figure 9 (left) describes the reachable behavior of the pair of FSA shown in Figure 10. Here, we see that the first variable in the

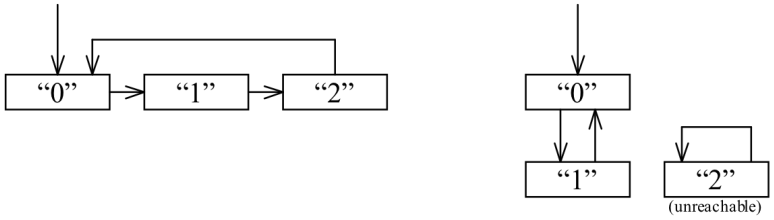

Figure 10: FSAs whose product is the FSA of Figure 9.

state of the FSA in Figure 9 (left) is the entire state for the first (left) FSA shown in Figure 10. Of course, the second variable in the state of the FSA in Figure 9 (left) is the state of the second (right) FSA from Figure 10. These two sub-states have already been concatenated to make the state of the FSA in Figure 9.

The FSA in Figure 9 (left) may be encoded as the relation shown in Figure 9 (right). We may then, for each tuple, concatenate the variable values from the corresponding elements, to produce the following set: { “0001”, “0010”, “0100”, “0111”, “1011”, “1020”, “1110”, “1121”, “2000”, “2021”, “2101”, “2120” }. We can then build a table of booleans to represent this set, after listing the domain in the first column:

“0000”	0
“0001”	1
“0002”	0
“0010”	1
“0011”	0
“0012”	0
“0020”	0
“0021”	0
“0022”	0
“0100”	1
“0101”	0
“0102”	0
“0110”	0
“0111”	1
“0112”	0

(cont.)	
“0120”	0
“0121”	0
“0122”	0
“0200”	0
“0201”	0
“0202”	0
“0210”	0
“0211”	0
“0212”	0
“0220”	0
“0221”	0
“0222”	0
“1000”	0
“1001”	0

(cont.)	
“1002”	0
“1010”	0
“1011”	1
“1012”	0
“1020”	1
“1021”	0
“1022”	0
“1100”	0
“1101”	0
“1102”	0
“1110”	1
“1111”	0
“1112”	0
“1120”	0

(cont.)	
“1121”	1
“1122”	0
“1200”	0
“1201”	0
“1202”	0
“1210”	0
“1211”	0
“1212”	0
“1220”	0
“1221”	0
“1222”	0
“2000”	1
“2001”	0
“2002”	0

(cont.)	
“2010”	0
“2011”	0
“2012”	0
“2020”	0
“2021”	1
“2022”	0
“2100”	0
“2101”	1
“2102”	0
“2110”	0
“2111”	0
“2112”	0
“2120”	1
“2121”	0

(cont.)	
“2122”	0
“2200”	0
“2201”	0
“2202”	0
“2210”	0
“2211”	0
“2212”	0
“2220”	0
“2221”	0
“2222”	0

The MDD that represents this set has already been shown in Figure 3.

2.3.3 Interleaved Decision Diagram representation of relations

The use of sets of pairs, to represent relations, similarly to the above description, may be implemented in other ways. One other way to obtain a representation of the value of a tuple is to shuffle, or *interleave*, the values of the variables belonging to all the elements of the tuple.

Here we take the set of tuples representing the previously described transition relation:

{ ⟨ “00” → “01” ⟩, ⟨ “00” → “10” ⟩, ⟨ “01” → “00” ⟩, ⟨ “01” → “11” ⟩, ⟨ “10” → “11” ⟩, ⟨ “10” → “20” ⟩, ⟨ “11” → “10” ⟩, ⟨ “11” → “21” ⟩, ⟨ “20” → “00” ⟩, ⟨ “20” → “21” ⟩, ⟨ “21” → “01” ⟩, ⟨ “21” → “20” ⟩ },

and in each case perform a perfect shuffle on the two variable values from the domain and the two variable values from the range, producing a single parameter with four variables, yielding the following set:

{“0001”, “0100”, “0010”, “0111”, “1101”, “1200”, “1110”, “1211”, “2000”, “2201”, “2011”, “2210”}.

This can easily be recognized as the same set in the caption of Figure 4, and results in the same small MDD representation. Inspection of the related tables and diagrams allows one to see how the first variable and the third variables in the MDD from section 2.2.2 are related to each other. They originate as the state variable in the FSA in Figure 10 (left), as incorporated as the first variable in the state of the FSA of Figure 9. The state transition relation, of that FSA, then incorporates the state same variable in both its domain and its range, producing related variables (the first and third variables) in the set-of-tuples encoding of that relation. Similarly, the second and fourth variables in the MDD from section 2.2.2 originate as the state variable in the FSA in Figure 10 (right), and are similarly incorporated into the domain and range, of the state transition relation of the FSA of Figure 9.

Thus, we can see from this example that the use, of interleaved representation of relations brings certain related variables together, in the MDD representation. This provides some of the benefits of good variable ordering

without a (potentially costly) variable re-ordering step, in the production of the final MDD.

2.3.4 Representation of functions of states using Decision Diagrams

We have seen that EV$^+$MDDs, EV*MDDs, and AADDs each can be used to efficiently represent certain real functions of states (and certain integer functions of states, as special cases). Any finite domain can be represented as sets of integers, consequently these types of decision diagrams can represent a broad range of functions.

Although we have used boolean functions to represent relations, it should be noted for the sake of completeness, that in set theory, functions are a kind of relation where each element of the domain is the first member of exactly one tuple. Consequently, functions of states, whose ranges are representable using decision diagrams, can be represented using decision diagrams in the same manner as the corresponding relation. Although it frequently happens that a state transition relation happens to be a function, it is typical for these functions to be represented in the same manner as are general relations.

2.4 Bisimulation

There are a variety of applications for bisimulation (see [13] for an overview of work in this area). Bisimulation[13] is used in definitions of equivalent computations in various models of concurrent computation, and also has applications such as FSA minimization and logic synthesis. In this work, we are primarily concerned with algorithmic aspects.

A bisimulation of a FSA is a binary relation among its states, and it is an equivalence relation. Any two states in this relation are observationally equivalent, in the sense that an FSA in one state cannot be distinguished from the FSA in the other state. Both states have the same sets of transitions enabled, and upon execution of the same transition, both FSA transition to new states that are also in the bisimulation. Thus, if any device, or simulation, was constructed to operate according to the rules of the FSA, one could not distinguish between two states in a bisimulation, by external observations or communication with the device. Devices whose FSA models have large bisimulations are therefore likely to have more states than necessary to implement their behavior. Fortunately, the size of the largest bisimulation indicates the size of the smallest equivalent FSA model having the same bahavior.

2.5 Relational coarsest partition

The relational coarsest partition of the state space of an FSA corresponds to the largest bisimulation of that FSA. It is a partition of the state space of the FSA, where the members, of any partition element, are all extensionally indistinguishable from each other.

The relational coarsest partition problem can be stated as follows:

Given a finite state machine (FSA), M, comprising a set of reachable states (nodes), a transition relation, a node coloring and an edge coloring (transition labels), determine the smallest (in number of states) finite state machine, M' equivalent to M. This equivalence can be formalized as follows:

The finite state machine $M = \langle S, Q, N, A\rangle$ (state space, transition relation, node colors, arc colors), where $Q \subseteq S \times S$, $N \in S \to color$, $A \in Q \to color$, has a smallest equivalent machine $M' = \langle S', Q', N', A'\rangle$ if and only if

1. There is a bijection F giving a correspondence between members of S' and a partition P of S, where: $\exists P \subseteq 2^S : (\bigcup P = S) \wedge (\forall p_1, p_2 \in P : p_1 = p_2 \vee p_1 \cap p_2 = \emptyset) \wedge \exists F \in (P \leftrightarrow S') :$

2. Members of Q' have the same color as each of the members of the corresponding partition in P and:

   $[\forall p \in P, s \in p, s' \in S' : F(p, s') \rightarrow (N(s) \leftrightarrow N(s'))] \wedge$

3. Transitions between members of S' correspond to transitions between members of the corresponding partitions in P, and have the same color

   $[\forall \langle p_1, s'_1 \rangle \in F, \langle p_2, s'_2 \rangle \in F, s_1 \in p_1, s_2 \in p_2 : (\langle s_1, s_2 \rangle \in Q \leftrightarrow \langle s'_1, s'_2 \rangle \in Q' \wedge A(\langle s_1, s_2 \rangle) = A'(\langle s'_1, s'_2 \rangle))]$

4. And there is no smaller M' with the same properties.

   Algorithms for solving this problem are discussed in the section on related work, and in the section describing our work.

2.6 Markov Models and Lumping

The solution to the relational coarsest partition problem in this work is motivated by its possible future extension to the Markov model lumping problem.

Lumping can be used to simplify a Markov model prior to calculating solutions for it. A typical use of Markov models involves calculating the expected value of the reward, where a finite state machine, M, is given, along with an initial state, transition probabilities, and a reward function over the states of M. Typically this is to be determined relative to the expected steady-state of the system. The reward function is usually a function whose range is some finite set of real values. This problem is usually solved by first using a linear system to calculate the steady-state probability of each state, then using the reward function to calculate the expected reward.

The (usually large) set of reachable states S may be represented by decision diagrams. Since the corresponding linear system may be prohibitively large, even when represented using decision diagrams, one may attempt to reduce the size of the system by using the "relational coarsest partition" of the system. The idea behind this, is that there may be collections of equivalent states in S, such that some smaller state machine, M', where individual states in M' correspond to collections (lumps) of states in M, has the same expected steady-state reward as M. This is frequently the case with state machines generated to model verification problems, and the use of "lumping" has become an important tool enabling the feasible solution of such systems. Algorithms to find such "lumped" systems M' are called "lumping algorithms" and are similar to DFA minimization algorithms.

The lumping problem is the problem of finding the smallest Markov model that is an equivalent refinement of a given Markov model. The notion of equivalent refinement can be formalized as follows:

One system, $M = \langle St, Pr, Re, In \rangle$ (the states, transition probability, reward, initial state), where $Pr \in St \times St \rightarrow \mathbb{R}$, and $Re \in St \rightarrow \mathbb{R}$, and $In \in St$ is refined to an "equivalent" system $M' = \langle St', Pr', Re', In' \rangle$ iff each of the following holds:

1. The members of St' correspond to members of a partition L of St, via some bijection F,

   $\exists L \subseteq 2^{St} : (\cup L = St) \wedge (\forall l_1, l_2 \in L : l_1 = l_2 \vee l_1 \cap l_2 = \emptyset) \wedge \exists F \in (L \leftrightarrow St') :$

2. The probability of transition from a state in one partition element to any state in some second (not necessarily distinct) partition element is the probability of transition between the corresponding members of St',

$[\forall E_1, E_2 \in L : \forall s_1 \in E_1 : (\sum_{s_2 \in E_2} Pr(s_1, s_2)) = Pr'(F(E_1), F(E_2))] \wedge$

3. The reward of any member of a partition element is the reward of the corresponding member of St',
   $[\forall E \in L : \forall e \in E : Re(e) = Re'(F(E))] \wedge$
4. And the initial state corresponds to the partition containing the original initial state.
   $[\exists E \in L : In \in E \wedge F(E) = In']$

Lumping algorithms typically focus on the construction of the partition L, starting with a coarse approximation that only satisfies (3) and (4) above. Refinement steps identify elements E_1 of L having members that do not satisfy (2) with respect to some specific E_2 (called the splitter), then replace E_1 in L with multiple elements whose union is E_1, and which do satisfy (2) with respect to that E_2.

It should be noted that, in the non-stochastic version of this problem, all rates are either 1 or 0. In this case, the matrix of rates becomes an adjacency matrix of a graph, and the problem reduces to the relational coarsest partition problem. The section on related work discusses Paige and Tarjan's algorithm [14], which performs lumping efficiently, given the graph representation of that problem.

3 Main Idea

The main idea (due to Ciardo [1]), implemented in this work, is the use of interleaved diagrams to represent the partition of the state space into equivalence classes. We expect this to yield space savings compared to non-interleaved representations, since existing non-interleaved representations are explicit in the number of equivalence classes found. We additionally expect improvement in execution time for the algorithms that use these representations, due to their manipulation of smaller structures. By reduction of memory and processing requirements, we hope to enable the processing of FSAs that could not be processed by previous methods. The primary motivation behind this idea is to provide the benefits of interleaved representation of partitions to the lumping problem. It appears [10] [6] [7] [4] [5] that this idea has not yet been applied to the lumping problem.

4 Related Work

The related work is divided into two parts. The work related only to Markov Lumping is given in a later section, as it pertains primarily to motivation and future work. As the present work was not applied to Markov lumping, only the work related to bisimulation is described in this section.

4.1 *Three partition refinement algorithms* [14]

This Article by Paige and Tarjan [14], describes their $O(m(log(n)))$ time algorithm for Relational coarsest partition. (where m = number of edges, n= number of vertices).

The main idea is to do iterative "splitting" on a sequence of partitions of the graph of the state space U. Each iteration splits partition members, each called B, using another partition member S, called the splitter. In the

[1] unpublished communication

new algorithm, S is either the entire set U, or S is chosen so that it is a subset of a previous splitter S_0 and at most half the size of S_0. Splitting B using S yields up to 3 subsets, B_0, and B_1, and B'. B_0 contains members of B with edges to S and no edges to $S_0 - S$. B_1 contains members of B with edges to both S and $S_0 - S$. B' contains members of B with only edges to $S_0 - S$. Using a fairly simple backward adjacency list representation, members of $B_0 \cup B_1$ can easily be identified in time linear with the number of edges from $B_0 \cup B_1$ to S.

A naive algorithm would also traverse the representation of $S_0 - S$, to identify the members of B', and to distinguish the members of B_0 from those of B_1. A major contribution of this paper is a method of associating edge counts with the vertices of B, of the number of edges to vertices of S, and maintaining them. The use of these edge counts allows for the identification of members of B_0 and of B_1 in time linear with the number of edges from $B_0 \cup B_1$ to S. After moving the vertices of B_0 and B_1 out of the representation of B, the part that remains in B now becomes the representation for B', so there is no need to explicitly identify the individual members of B' as part of the splitting process. These simplifications allow the overall iterative splitting algorithm to achieve the $O(m(log(n)))$ bound.

The edge counts are maintained and used as follows. An edge count data structure exists for each pair of a member of U, and potential splitter S. Each data structure representing an edge from a member of U to a member of S also contains a pointer to the corresponding edge count data structure, which represents the number of such edges. Whenever S is itself split, usually the data structures representing S will be re-used to represent one of the largest products of such a split, while new data structures will be used to represent the other products. The edge count data structures will be updated while updating edges pointing to members of S that are moved to other products.

When splitting B on splitter S, we traverse reverse adjacency lists of members of S to determine members of $B_0 \cup B_1$. We will re-use data structures representing S_0, to represent $S_0 - S$, and reuse structures representing B, to represent B'. Consequently, it will be unnecessary to explicitly identify members of B'. When traversing reverse adjacency lists of members of S to determine members of $B_0 \cup B_1$, we also count how many edges occur, from each member of $B_0 \cup B_1$, to members of S. After this traversal, the members of B_0 and members of $B_0 \cup B_1$ can easily be distinguished, since the counts for members of B_0 (but not of B_1) will be identical to the edge counts for the member of edges pointing to S_0.

For analysis purposes, observe that any given element of U can only occur as a member of a splitter, up to $O(log(n))$ times, since a splitter S is always chosen to be, at most, half the size of S_0, a previous splitter containing S. Observing that each splitting operation is performed by traversing reverse adjacency lists of elements of a splitter, so that each element contributes cost linear in the size of its adjacency list each time it occurs in a splitter, we derive the overall $O(m(log(n)))$ bound.

4.2 *Symbolic Bisimulation Minimisation* [1]

This (1992) article by Amar Bouali and Robert De Simone describes an algorithm that is nearly the same as the present algorithm. The main purpose of their algorithm is to calculate *weak bisimulation*, a form of bisimulation where some transitions are considered to be unobservable. They transform a weak bisimulation problem in to the standard bisimulation problem by pre-processing the collection of transition relations. They perform a comparison of their algorithm using only interleaved decision diagrams, with their algorithm using only non-interleaved diagrams. Our purpose, is to evaluate the use of interleaved diagrams for storage of the equivalence relation, to gauge feasibility of using this technique for lumping. Consequently, we compare this algorithm using only interleaved decision diagrams, with a new algorithm using interleaved decision diagrams for transition relations, but also using

non-interleaved decision diagrams for the equivalence relation. In this way, our comparison is more focused on the representation of the equivalence relation.

4.3 *An efficient algorithm for computing bisimulation equivalence*[8]

This (2004) algorithm by Agostino Dovier, Carla Piazza, and Alberto Policriti operates by first producing a (probably) good initial partition of the set of states, based on the calculated *rank* of states. They can do this because states with different rank cannot be equivalent. For their non-symbolic implementation, they use the set-theoretic notion of rank. The possible presence of cycles in a state transition graph forces them to use non well-founded set theory. In order to compute rank symbolically, they adjust the definition of rank, so that, for many states, rank is essentially the longest distance from the state to a final state through the transition graph after all cycles have been condensed to a single state. Fortunately, they are able to show that their algorithm always terminates in a linear number of symbolic steps. After their initial partitioning based on rank, other algorithms must be used to finish the partitioning. The rank sequence of the initial partition can be used to efficiently direct the ordering of splitting operations.

4.4 *Forwarding, Splitting, and Block Ordering to Optimize BDD-based Bisimulation Computation*[19]

This (2007) paper by Ralf Wimmer, Marc Herbstritt, and Bernd Becker describes several methods to accelerate symbolic bisimulation computation. The main algorithm is similar to the one used in the current work, as well as in [1], although partition elements are represented explicitly, and assigned unique serial numbers. Aside from the complication of handling invisible transitions, the main optimizations they employ are as follows:

1. They use *signatures* of states to compute the refinements of partition elements (or blocks), as does the current work. States with different signatures will belong to different partition blocks. Their DD representation for signatures places the state variables toward the root, and the signature variables toward the leaves. This allows them to simply substitute block serial numbers into the DD at the level of the signature, to produce a refined partition efficiently, as the canonicity of the DD representation guarantees that each node at that level corresponds to a distinct block. This technique is also employed in [5].

2. *Block Forwarding* refers to the update of the current partition immediately after blocks are split. They split only one block at a time, so they need only calculate signatures one block at a time. Therefore, they update the partition after each block splitting, allowing subsequent splitting operations to benefit from the more refined partition immediately. This technique is also employed in [4].

3. *Split-Driven Refinement* refers to the use of a *backward signature* (similar to the inverse of the state transition relation) to determine which blocks may be made splittable by the splitting of a given block. This allows the algorithm to skip splitting certain blocks whose elements signatures do not include any blocks that have been split since the certain block was created.

4. *Block ordering* is the deliberate choice of which splitter to use at any given time that such a choice is available. They mention two heuristic orderings, both of which produce improved run times. The choice of the block with a larger backward signature, as well as the choice of the larger block, both produced improvements.

They cannot use interleaved variable ordering for their representation of partitions, since their block forwarding, splitting and ordering optimizations depend on explicit treatment of individual partition blocks. Interestingly, their "future work" section, mentions their intention to apply these techniques to stochastic bisimulations for Interactive Markov Chains.

5 Algorithms

In this section, the algorithms used in the current work are given, starting with the main relational coarsest partition algorithm, preceded by definitions used by various algorithms.

The algorithms are described in a manner independent of variable ordering. Consequently, the algorithms are not bifurcated in that way. In some cases, however, more than one version of an algorithm is given, either to illustrate a choice in optimization, or to show some structural choice.

5.1 Definitions

The following operator definitions will be used in various algorithms. It should be noted that we consider predicates (relations) to be sets of tuples, so that we use predicate notation "$F(x, y)$" interchangeably with set notation "$\langle x, y\rangle \in F$" in much of the following:

(parameters a, b, c, x, y are states, while F, G are predicates over, or sets of, states):

$DC_1(F, G) \triangleq F'$, where $F'(a, x, y) = F(x, y) \wedge G(a)$ inserts don't-care parameter (from G) into position 1

$DC_1(F, G) \triangleq F'$, where $F'(a, x, y, z) = F(x, y, z) \wedge G(a)$ inserts don't-care parameter (from G) into position 1

$DC_2(F, G) \triangleq F'$, where $F'(x, a, y, z) = F(x, y, z) \wedge G(a)$ inserts don't-care parameter (from G) into position 2

$DC_2(F, G) \triangleq F'$, where $F'(x, a, y) = F(x, y) \wedge G(a)$ inserts don't-care parameter (from G) into position 2

$DC_2(F, G) \triangleq F'$, where $F'(x, a) = F(x) \wedge G(a)$ inserts don't-care parameter (from G) into position 2

$DC_3(F, G) \triangleq F'$, where $F'(x, y, a) = F(x, y) \wedge G(a)$ inserts don't-care parameter (from G) into position 3

$DC_3(F, G) \triangleq F'$, where $F'(x, y, a, z) = F(x, y, z) \wedge G(a)$ inserts don't-care parameter (from G) into position 3

$DC_4(F, G) \triangleq F'$, where $F'(x, y, z, a) = F(x, y, z) \wedge G(a)$ inserts don't-care parameter (from G) into position 4

$F^{-1}(y, x) \triangleq F(x, y)$ switch variables

$proj_{\vee 2}(F) \triangleq F'$, where $F'(x, y, z) = \bigwedge a : F(x, a, y, z)$ project second parameter by disjunction

$proj_{\vee 3}(F) \triangleq F'$, where $F'(x, y) = \bigvee a : F(x, y, a)$ project third parameter by disjunction

$(F \cap G)(\ldots args \ldots) \triangleq (F(\ldots args \ldots) \wedge G(\ldots args \ldots))$ intersection

$(F \cup G)(\ldots args \ldots) \triangleq (F(\ldots args \ldots) \vee G(\ldots args \ldots))$ union

$(\overline{F})(\ldots args\ldots) \triangleq \neg(F(\ldots args\ldots))$ complement

$(F \cup G)(\ldots args\ldots) \triangleq (F(\ldots args\ldots) \neq G(\ldots args\ldots))$ states in F or G but not both ($= (F \setminus G) \cup (G \setminus F)$)

Within algorithms, script letters ($\mathcal{E}$, $\mathcal{Q}$, $\mathcal{S}$, $\mathcal{T}$) will be used in names of BDD representations of sets and relations.

Efficient recursive algorithms for computing $(F \cap G)$, $(F \cup G)$, $(\overline{F})$, $(F \setminus G)$, and $|F|$ using caches, are well known, and are provided by the SMART MDD library.

Algorithms for computing $proj_{\vee 2}$, $proj_{\vee 3}$ (existential quantification), $\bigcup_i F_i$ (unions of many sets), and $DC_n(\ldots)$ (insertion of don't-care parameters), are described below, after the main algorithm.

5.2 Fixed-point minimization algorithm

This is the main algorithm for relational coarsest partition. It is essentially the same algorithm as that used by Bouali and De Simone [1].

Given representations of the following components of a labeled transition system:

$S \triangleq$ The state space of the system.

$Q_t(a,b) \triangleq$ (a transition from a to b exists, with label t) The transition matrix of a graph, and:

$E(a,b) \triangleq$ (a and b are in the same class) An existing partition of the same graph,

Define a function $E' = Refine(E)$ as follows:

$E'(a,b) = E(a,b) \wedge \Delta E(a,b)$, where:

$\forall t : T_t(a,b) = \bigvee c : (Q_t(a,c) \wedge E(b,c))$ a transition (labeled t) exists from a to b's equivalence class

$\Delta E(a,b) = \bigwedge t : \bigwedge c : (T_t(a,c) = T_t(b,c))$ a and b have the same transitions to the same equivalence classes.

Finally, starting with an initial partition based on state labels, $E_0(s_1,s_2) =$ (s_1 and s_2 have the same state label), Calculate the closure of $Refine$ on E_0, yielding $E_{n_{max}} = Refine(E_{n_{max}})$, where $E_{n+1} = Refine(E_n)$.

E_0 is the equivalence relation for the relational coarsest partition of the given labeled transition system.

Algorithm 1:

MDD *Refine*($\mathbb{N}\ \mathcal{N}_{transition\_labels}$, MDD $\mathcal{Q}_{[]}$, MDD $\mathcal{E}$, MDD $\mathcal{S}$) is
local MDD $\mathcal{T}_{[]}$, MDD $\overline{\Delta\mathcal{E}}$, MDD $\mathcal{E}'$,

1 $\overline{\Delta\mathcal{E}} \leftarrow \emptyset$
2 for $t \in [0, \mathcal{N}_{transition\_labels})$ loop
3 $\mathcal{T}_t \leftarrow proj_{\vee 3}((DC_2(\mathcal{Q}_t, \mathcal{S})) \cap (DC_1(\mathcal{E}, \mathcal{S})))$ • $\mathcal{T}_t(a,b) = \bigvee c : (\mathcal{Q}(a,c) \wedge \mathcal{E}(b,c))$
4 $\overline{\Delta\mathcal{E}} \leftarrow \overline{\Delta\mathcal{E}} \cup proj_{\vee 3}(DC_2(\mathcal{T}_t, \mathcal{S}) \uplus DC_1(\mathcal{T}_t, \mathcal{S}))$ • $\Delta\mathcal{E}(a,b) = \bigwedge t \in [0,t] : \bigwedge c : (\mathcal{T}_t(a,c) = \mathcal{T}_t(b,c))$
5 end loop
6 $\mathcal{E}' = \mathcal{E} \setminus \overline{\Delta\mathcal{E}}$ • $\mathcal{E}' = \mathcal{E} \cap \Delta\mathcal{E}$
7 return $\mathcal{E}'$

```
MDD RefineClosure( ℕ 𝒩_transition_labels, MDD 𝒬_[], MDD 𝒮, ℕ 𝒩_state_labels, MDD 𝒮ℒ_[] ) is
  local MDD ℰ_0, MDD ℰ, MDD ℰ_old,
  1  ℰ_0 ← ∅                                                          • Construct initial partition ℰ_0
  2  for l ∈ [0,𝒩_state_labels) loop
  3    ℰ_0 ← ℰ_0 ∪ DC_2(𝒮ℒ_l, 𝒮ℒ_l)
  4  end loop
  5  ℰ ← ℰ_0                                                          • ℰ(a,b) = ∃l ∈ [0,𝒩_state_labels) : (a ∈ 𝒮ℒ_l ∧ b ∈ 𝒮ℒ_l)
  6  repeat                                                           • ℰ ← Refine( ℰ ) until ℰ = Refine( ℰ )
  7    ℰ_old ← ℰ
  8    ℰ ← Refine( 𝒩_transition_labels, 𝒬_[], ℰ, 𝒮 )
  9  until ℰ = ℰ_old
  10 return ℰ                                                         • E_{n_max}
```

Algorithm 1, Closure of partition refinement.

In practice, both algorithms are integrated, and we don't use state labels. Consequently, as implemented, our algorithm is more similar to the following:

Algorithm 1.1:

```
MDD RefineClosure( ℕ 𝒩_transition_labels, MDD 𝒬_[], MDD 𝒮 ) is
  local MDD ℰ, MDD ℰ_old, MDD 𝒯_[], MDD Δℰ
  1  ℰ ← DC_2(𝒮,𝒮)                                                   • ℰ(a,b) = a ∈ 𝒮 ∧ b ∈ 𝒮
  2  repeat                                                           • ℰ ← Refine( ℰ ) until ℰ = Refine( ℰ )
  3    ℰ_old ← ℰ
  4    Δℰ ← ∅
  5    for t ∈ [0,𝒩_transition_labels) loop
  6      𝒯_t ← proj_∨3((DC_2(𝒬_t,𝒮)) ∩ (DC_1(ℰ,𝒮)))                   • 𝒯_t(a,b) = ⋁ c : (𝒬(a,c) ∧ ℰ(b,c))
  7      Δℰ ← Δℰ ∪ proj_∨3(DC_2(𝒯_t,𝒮)⊎DC_1(𝒯_t,𝒮))                  • Δℰ(a,b) = ⋀ t ∈ [0,t] : ⋀ c : (𝒯_t(a,c) = 𝒯_t(b,c))
  8    end loop
  9    ℰ = ℰ \ Δℰ                                                     • ℰ = ℰ ∩ Δℰ
  10 until ℰ = ℰ_old
  11 return ℰ                                                         • E_{n_max}
```

Algorithm 1.1, Closure of partition refinement.

With the integrated implementation, it becomes a simple matter to describe Forwarding:

Algorithm 1.2:

```
MDD RefineClosure( ℕ 𝒩_transition_labels, MDD 𝒬_[], MDD 𝒮 ) is
  local MDD ℰ, MDD ℰ_old, MDD 𝒯_[], MDD Δℰ
  1  ℰ ← DC_2(𝒮,𝒮)                                                   • ℰ(a,b) = a ∈ 𝒮 ∧ b ∈ 𝒮
  2  repeat                                                           • ℰ ← Refine*( ℰ ) until ℰ = Refine( ℰ )
  3    ℰ_old ← ℰ
  4    for t ∈ [0,𝒩_transition_labels) loop
  5      𝒯_t ← proj_∨3((DC_2(𝒬_t,𝒮)) ∩ (DC_1(ℰ,𝒮)))                   • 𝒯_t(a,b) = ⋁ c : (𝒬(a,c) ∧ ℰ(b,c))
  6      Δℰ ← proj_∨3(DC_2(𝒯_t,𝒮)⊎DC_1(𝒯_t,𝒮))                      • Δℰ(a,b) = ⋀ c : (𝒯_t(a,c) = 𝒯_t(b,c))
  7      ℰ = ℰ \ Δℰ                                                  • ℰ = ℰ ∩ Δℰ (update ℰ for use by next iteration of inner loop)
  8    end loop
  9  until ℰ = ℰ_old
  10 return ℰ                                                         • E_{n_max}
```

Algorithm 1.2, Closure of partition refinement, with forwarding.

In the *Refine* algorithm, the objective is to construct a refinement of the existing partition. We represent the partition as an binary equivalence relation $\mathcal{E}$, among members of $\mathcal{S}$, the state space, so that any two members of the same partition block, will occur in a pair of the relation $\mathcal{E}$. Since unlabeled states can only be distinguished by which states are the targets of their transitions, we compose a state transition relation $\mathcal{Q}_t$ and the partition equivalence relation $\mathcal{E}$. This composition $\mathcal{T}_t$ is described on line 3. The relation $\mathcal{T}_t = \{\langle a, b\rangle | \bigvee c : (\mathcal{Q}_t(a,c) \wedge \mathcal{E}(b,c))\}$, is clearly a composition of $\mathcal{Q}_t$ and $\mathcal{E}^{-1}$, since whenever $\mathcal{T}_t(a,b)$, $\mathcal{Q}_t(a,c) \wedge \mathcal{E}^{-1}(c,b)$ for some c. Since $\mathcal{E}$ is an equivalence relation, $\mathcal{E} = \mathcal{E}^{-1}$, therefore we have $\mathcal{T}_t = \mathcal{Q}_t \circ \mathcal{E}$. The meaning of $\mathcal{T}_t(a,b)$ is that state a has a transition to the equivalence class containing b.

In the final partition $E_{n_{max}}$, two states a and b will be distinguishable (be in separate partition classes) if they do not have transitions to the same set of partition classes. We would therefore like to know when two states have transitions to the same partition classes, according to the current partition $\mathcal{E}$. So, in line 4, we construct $\overline{\Delta\mathcal{E}}$ for this purpose. $\overline{\Delta\mathcal{E}}(a,b)$ holds only if a and b have some difference c in the classes to which they transition. This is clearly the case, by definition of $\cup$, $\overline{\Delta\mathcal{E}}(a,b)$ implies $\mathcal{T}_t(a,c) \neq \mathcal{T}_t(b,c)$, for some c. This means that either a has a transition to cs equivalence class and b does not, or that b has a transition to cs class and a does not. $\overline{\Delta\mathcal{E}}$ therefore accumulates pairs of states we are determining do not belong in the same class. We then refine $\mathcal{E}$ to be more like $E_{n_{max}}$ in line 6 of *Refine*, by removing from it those pairs of states accumulated in $\overline{\Delta\mathcal{E}}$.

In the *RefineClosure* algorithm, lines 1-4 construct the initial partition $\mathcal{E}_0$ based on the state labels. Lines 6-9 iteratively refine the current partition, until the termination condition, $\mathcal{E} = \mathcal{E}_{old} = \mathit{Refine}(\ \mathcal{E}_{old}\ )$, is met. Since the initial partition is finite, and the *Refine* algorithm operates by removing members of $\mathcal{E}$, *RefineClosure* is guaranteed to terminate. The termination condition $\mathcal{E} = \mathit{Refine}(\ \mathcal{E}\ )$ guarantees that upon termination, $\mathcal{E}$ meets requirements 1, 2, and 3 listed above, for relational coarsest partition. Showing that requirement 4 is met is beyond the scope of this current writing.

Algorithm 1.1 changes *RefineClosure* to incorporate the content of *Refine*, while algorithm 1.2 applies forwarding to the closure loop. Here, $\mathcal{E}$ is updated on line 7 in the inner loop. Consequently, the calculations on lines 5 and 6 in the next iteration can benefit from using the recently updated value of $\mathcal{E}$.

5.3 Algorithm for $proj_{\vee 3}$ (existential quantification)

Here is our algorithm to calculate a binary relation $F' = proj_{\vee 3}(F)$, by projecting a parameter from a 3-ary relation F, such that $F'(x,y) = \bigvee a : F(x,y,a)$.

Given a (possibly) interleaved DD representing a set F, produce an DD representing the projection/quantification $F' = \vee F$ of F, satisfying the following:

$(\vee F)(x,y) \triangleq \bigvee a : F(x,y,a)$ project third variable by disjunction)

We will divide the nodes of the graph representing F into three classes:

1. ordinary nodes, at the level of variables of parameter x, not quantified over
2. ordinary nodes, at the level of variables of parameter y, not quantified over
3. reducible nodes, at the level of variables of parameter a, being existentially quantified

We will assume that (the data structure for) each node is identifiable in constant time as either ordinary or reducible.

Additionally, we will assume that there are no nodes which represent empty sets; Only NULL edges will be used to represent empty sets, which can be identified in constant time.

The following recursive algorithm is functionally equivalent to a non-recursive algorithm that starts at the leaf level, and while proceeding toward the root, performs (recursive) union projections on reducible nodes. The recursive implementation is unavoidable, as our BDD package only supports the functional style, that is, it does not support mutation of existing structures. Its helper function *operateUnion*, is described in the next subsection.

Algorithm 2:

```
MDD projectUnion( MDD F ) is
  local  MDD  G
  local  MDD  H
  local  MDD  R
   1 if F = ∅ then return ∅;                                   • handle empty set
   2 if F is a leaf then return F;                             • handle trivial (leaf) case (true or false)
   3 if projectUnion( F ) is found in the cache, return projectUnion( F )
   4 construct a new node G as follows:                        • G ← node where child i = projectUnion( child i of F )
   5   for each edge slot H in F with index i
   6     place projectUnion( H ) into G with index i
   7   G ← unique( G )                                         • use unique table
   8 if F references an ordinary node then
   9   R ← G
  10 else F is not ordinary ... F is reducible
  11   R ← operateUnion( G )                                   • takes the union of all Gs children
  12 endif
  13 place R = projectUnion( F ) into cache
  14 return R
```

Algorithm 2, existential quantification to project out all reducible nodes

Lines 4-6 of this algorithm directly access the children of the input tree. Due to the cache memoization, this algorithm efficiently does a depth first traversal of the input tree, copying the subtree as it proceeds. Whenever the depth first traversal is leaving a "reducible" node, the reduction is processed by calling the *operateUnion* function on line 11.

5.4 Algorithm for calculating $\bigcup_i F_i$ (unions of many sets)

This algorithm to union many sets, represented as MDDs, attempts to make good use of the union cache. The general problem of how to optimally use the union cache is a hard one. Here we use a simple greedy algorithm, that depends on an ordering of MDDs. We attempt to take unions of "near" MDDs before other unions, and hopefully populate the union cache with unions we are likely to re-use.

Algorithm 3:

```
MDD operateUnion( MDD S ) is                                   • members of S only have ordinary nodes
  local  sorted MDD list  H[]                                  • any consistent total ordering will do, we use node address
  local  ℕ  n
   1 if S = ∅ then return ∅
   2 forall s ∈ children of S, insert s into H                  • put Ss children into a sorted list
   3 main loop:
   4 while length(H) > 1 loop
   5   n ← length(H)
   6   remove duplicates from H
   7   if duplicates were found, then continue with next iteration of main loop
   8   if ∃l ∈ [1,n) : ∃i ∈ [1,n−l] : H[i] ∪ H[i+l] is in cache, then   • try to use union cache
   9     let l be smallest such l, and then let i be smallest such i   • prefer unions of closer elements
  10     remove H[i] and H[i+l] from H, but insert H[i] ∪ H[i+l] from cache
  11     continue with next iteration of main loop
  12   end if
  13   remove H[1] and H[2] from H, but insert H[1] ∪ H[2]
  14 end loop
  15 return H[1]                                                 • the one remaining element
```

Algorithm 3, union of many MDDs.

We attempt to take the union of all children of the input MDD in a manner that takes maximum advantage of the union cache, which stores the results of various past union operations. In line 8 we attempt to find union cache entries that will provide partial results for this calculation. By using a sorted list and by the conditions on line 9 we attempt to evaluate unions, that may be relatively easy to re-use in some later invocation. It is believed that duplicate entries occur frequently. Using a sorted list allows the removal of duplicates on line 6 to occur efficiently, and thereby avoid unnecessary work.

5.5 Algorithm for calculating $DC_n(\ldots)$ (insertion of don't-care parameters)

This algorithm is used to introduce don't-care variables into the decision diagram representation of a relation.

There is a parameter F giving the relation. Even don't-care variables must belong to some specific set, so there is also a parameter G, giving the set from which the don't-care variables values are drawn. Our algorithm description gives no explicit parameter to designate the levels into which the don't care variables are inserted (although our actual code does). As described here, our algorithm solves the following problem:

Given decision diagrams representing relations F and G, construct a (possibly interleaved) diagrams representing relation F', where

$F'(\ldots$ f-variables and g-variables $\ldots) = F(\ldots$ f-variables $\ldots) \wedge G(\ldots$ g-variables $\ldots)$

This is a generalization that covers all the cases:

$F'(a,x,y) = F(x,y) \wedge G(a)$ inserts don't-care parameter (from G) into position 1 ($DC_1(F,G)$)

$F'(a,x,y,z) = F(x,y,z) \wedge G(a)$ inserts don't-care parameter (from G) into position 1 ($DC_1(F,G)$)

$F'(x,a,y,z) = F(x,y,z) \wedge G(a)$ inserts don't-care parameter (from G) into position 2 ($DC_2(F,G)$)

$F'(x,a,y) = F(x,y) \wedge G(a)$ inserts don't-care parameter (from G) into position 2 ($DC_2(F,G)$)

$F'(x,a) = F(x) \wedge G(a)$ inserts don't-care parameter (from G) into position 2 ($DC_2(F,G)$)

$F'(x,y,a) = F(x,y) \wedge G(a)$ inserts don't-care parameter (from G) into position 3 ($DC_3(F,G)$)

$F'(x,y,a,z) = F(x,y,z) \wedge G(a)$ inserts don't-care parameter (from G) into position 3 ($DC_3(F,G)$)

$F'(x,y,z,a) = F(x,y,z) \wedge G(a)$ inserts don't-care parameter (from G) into position 4 ($DC_4(F,G)$)

I assume that a diagram representing F' has L levels, and that L is also the sum of the total number of variables in Fs and Gs parameters.

We produce F' as follows: Let $F' \leftarrow DC(\ L,\ F,\ G\ )$,

where DC is computed as in:

Algorithm 4:

```
MDD DC( ℕ L, MDD F, MDD G ) is
  local  MDD  R
   1 if F = ∅ ∨ G = ∅, return ∅
   2 if DC( L, F, G ) is found in cache then return DC_n( L, F, G ) from cache
   3 if level L of the output is leaves, then                    • F and G will also be leaves
   4   R ← 1
   5 else if level L of the output corresponds to input parameter F then
   6   create a new MDD node R
   7   for each child f of F with index i, loop
   8     place a corresponding child DC( L − 1, f, G ) into R, with index i
   9   end loop
  10   end if
  11 else (level L of the output corresponds to parameter G)
  12   create a new MDD node R
  13   for each child g of G with index i, loop
  14     place a corresponding child DC( L − 1, E, g ) into R, with index i
  15   end loop
  16 end if
  17 R ← unique( R )
  18 place R = DC( L, F, G ) into cache
  19 return R
```

Algorithm 4, insertion of don't care variables.

This recursive layer-by-layer construction of the output MDD constructs each layer by considering which variable belongs in the current layer using the test on line 5. The current layer of F is copied to the output MDD by lines 6-10 for a layer whose variable belongs to input F. Lines 12-15 deal with the case where the variable of the current layer belongs to G. When we use a node from F or G, we descend to its child for the recursive call. Lines 3-4 describe the relatively trivial case for leaves. Given that F' has L levels, L being the total number of variables in Fs and G, we will recursively reach the leaves of Fs and G when they are needed for use on lines 3-4.

5.6 Number of equivalence classes in an interleaved equivalence relation

It is a relatively simple matter to calculate the number of equivalence classes in an equivalence relation represented in a non-interleaved manner. Here we give the algorithm we use to count equivalence classes in an interleaved

equivalence relation.

Given an interleaved decision diagram representing an equivalence relation $E \subseteq S \times S$, calculate the number $|\{\{x|E(x,y)\}|y \in S\}|$ of equivalence classes of E. Any total ordering $<$ can be used to associate to each block B, in E, some unique minimum element $b \in B$, $\forall c \in B : b \leq c$, so the problem can be reduced to counting the counting the minimum elements b, such that $\forall c \in B : b \leq c$, where $B = \{c|E(b,c)\}$. Hence, we actually calculate:

$N_E = |\{\ b \in S \mid \forall c \in \{c|E(b,c)\} : b \leq c\ \}|$

As our ordering relation $<$, we will use the lexicographic ordering of states. Now we define:

$(proj_{\vee 2}(F))(x) \triangleq \bigvee a : F(x,a)$ project second variable (of 2) by disjunction

$(selectNonMin(F))(b,c) \triangleq b \not\leq c \wedge F(b,c)$ select pairs where the first element is not minimal

$mag(F) \triangleq \Sigma_{x \in S|F(x)} 1$ magnitude of set

Using these definitions, the calculation can be performed as: $N_E \leftarrow mag(\ S \setminus proj_{\vee 2}(\ selectNonMin(E)\ )\ )$

We now give the algorithm for computing $selectNonMin(E)$. I assume that the variable levels in E occur in pairs, with the same ordering for both parameters of E, the variable from the domain being first (closer to the root), followed by the corresponding variable from the range, the most significant variables being toward the root.

Algorithm 5:

```
MDD selectNonMin( MDD E_b ) is
  local  MDD  R_b
  local  MDD  R_c
   1 if selectNonMin( E_b ) is in cache, return selectNonMin( E_b ) from cache
   2 if E_b is a leaf, then
   3   R_b ← ∅                                  • if we got here, the values are equal, so eliminate
   4 else                                       • not leaf
   5   R_b ← a new empty MDD node
   6   for each child E_c of E_b loop
   7     let b_0 be the value at this level for E_c within E_b in:
   8       R_c ← a new empty MDD node
   9       for each child E'_b of E_c loop
  10         let c_0 be the value at this level for E'_b within E_c in:
  11           if b_0 > c_0 then
  12             into R_c insert child E'_b, with value c_0
  13           else if b_0 = c_0 then
  14             into R_c insert child selectNonMin( E'_b ), with value c_0
  15           end if                           • insert nothing when b_0 < c_0
  16       end loop
  17       into R_b insert child unique( R_c ), with value b_0
  18   end loop
  19 end if
  20 R_b ← unique( R_b )
  21 place R_b = selectNonMin( E_b ) into cache
  22 return R_b
```

Algorithm 5, selection of non-minimum elements

The function selects the subset of the tree corresponding to the case where the variable on the even level has a

value b_0, greater than the value c_0 of the child on the odd level, taking two levels at a time as controlled by the loop statements on lines 6 and 9. If the inequality holds, as tested on line 11, the entire subtree is selected without further testing. If the opposite inequality holds, the entire subtree is rejected without further testing. Only in the case where the two values are equal as tested on line 13, the function is called recursively at line 14. There is therefore no way to arrive at a subtree, unless the values of variables considered at higher levels have occurred as equal up to this point. Therefore, when line 2 finds that the input is a leaf, line 3 can safely reject, since we are choosing to select for an inequality, while arriving at a leaf indicates equality of variable values.

5.7 Unified calculation of $(DC_2(Q,S)) \cap (DC_1(E,S))$, given $E \subseteq S \times S$

This algorithm produces the desired result $(DC_2(Q,S)) \cap (DC_1(E,S))$, without constructing any decision diagrams, such as $DC_2(Q,S)$ or $DC_1(E,S)$. This algorithm operates by syncronized recursive traversal of the structures representing the three inputs S, Q, and E as the output is constructed recursively.

Given decision diagrams representing a transition relation $Q \subseteq \hat{S} \times \hat{S}$, and an equivalence relation $E \subseteq S \times S$, this algorithm produces a decision diagram representing the unquantified composition $t = (DC_2(Q,S)) \cap (DC_1(E,S))$ of Q and E, limited to S. Expanding the definitions of DC_2 and DC_1, we see that:

$\forall a, b, c \in \hat{S} : t(a,b,c)$ iff $(Q(a,c) \wedge S(b)) \wedge (E(b,c) \wedge S(a))$

Since $E \subseteq S \times S$, $E(b,c)$ guarantees $S(b)$ (and $S(c)$), we may eliminate $S(b)$, deriving:

$\forall a, b, c \in \hat{S} : t(a,b,c)$ iff $Q(a,c) \wedge E(b,c) \wedge S(a)$

I assume that the variable levels in t and Q corresponding to parameters a and c occur in the same ordering, and also that the variable levels in t and E corresponding to parameters b and c occur in the same ordering.

Assume that a diagram representing S has L levels, a diagram representing Q or E has $2L$ levels and a diagram representing t has $3L$ levels.

We produce t as follows: Let $t \leftarrow$ *UcompL*($3L$, Q, E, S),

where *UcompL* is computed as in:

Algorithm 6:

```
MDD UcompL( ℕ N, MDD Q, MDD E, MDD S ) (memoized function) is
  local  MDD  R
 1 if UcompL( N, Q, E, S ) is found in cache, return UcompL( N, Q, E, S ) from cache
 2 if level N of the output is leaves, then                          • Q and E will also be leaves
 3   R ← Q ∩ E, using leaf rules
 4 else if level N of the output corresponds to parameter a then     • DC1(E) has a don't care at this level
 5   if Q = ∅ ∨ S = ∅ ∨ (Q and S have no children with same index) then R ← ∅, else:
 6     create a new MDD node R
 7     for each child q of Q and child s of S, having the same index, loop   • use only members of Q where a ∈ S
 8       place a corresponding child UcompL( N − 1, q, E, s ) into R
 9     end loop
10   end if
11 else if level N of the output corresponds to parameter b then     • DC2(Q) has a don't care at this level
12   if E = ∅ then R ← ∅, else:
13     create a new MDD node R
14     for each child e of E loop
15       place a corresponding child UcompL( N − 1, Q, e, S ) into R
16     end loop
17   end if
18 else (level N of the output corresponds to parameter c)
19   if Q = ∅ ∨ E = ∅ ∨ (Q and E have no children with same index) then R ← ∅, else:
20     create a new MDD node R
21     for each child q of Q and child e of E, having the same index, loop
22       place a corresponding child UcompL( N − 1, q, e, S ) into R
23     end loop
24   end if
25 end if
26 R ← unique( R )
27 place R = UcompL( N, Q, E, S ) into cache
28 return R
```

Algorithm 6, unquantified composition, limited to reachable states S.

As in algorithm 4, we recursively descend the input MDDs, choosing how to construct each level of the output, based on whose variables occur at that level. At each level, we clone the structure of each input MDD involved with the variable at that level, always using the intersection, in the case where more than one input MDD is involved. When ever we clone a level of an input, we descend to its children recursively when we descend to construct the next (lower) level of the output. Uninvolved input MDDs are passed unchanged to the recursive call that constructs a child at the next level.

Lines 2,4, and 11 determine the inputs of the variable at the current level of the output being constructed. Lines 5-10 clone the output layer from input MDDs Q and S, since the layer corresponds to a variable in parameter a. Note the recursive call on line 8 passes the children of the cloned inputs, but passes the other inputs directly. Similarly, lines 12-17 clone the output layer from E, since a variable from parameter b is represented at this level. And lines 19-24 clone from Q and E since a variable from parameter c is found. If all operates correctly, the leaf level of the output is found when the leaf levels of the inputs are present, So that this case can be handled by lines 2 and 3.

5.8 Hybrid fixed-point minimization algorithm

This algorithm for relational coarsest partition uses interleaved MDDs to represent the transition relations Q_t, while using non-interleaved MDDs to represent the partition E of the state space.

It is similar to algorithm 1.2, except for the part of the inner loop dealing with partition calculation.

Given representations of the following components of a labeled transition system:

$S \triangleq$ The state space of the system.

$Q_t(a,b) \triangleq$ (a transition from a to b exists, with label t) The transition matrix of a graph, and:

$E(a,k) \triangleq$ (a is in class numbered k) An existing partition of the same graph,

Define functions $E' = RefineH_t(E)$ as follows:

let $T_{partial(t)}(a,c,d) \triangleq \bigvee b : (Q_t(a,b) \wedge E(a,c) \wedge E(b,d))$ a transition (labeled t) exists from a (in class c), to some b, in class d

let $W(a,c,d) \triangleq E(a,c) \wedge d = 0$ a relation just like E, except with a third member $d = 0$, to match the form of $T_{partial(t)}$

let $T_t \triangleq T_{partial(t)} \cup W$ associate the signature $\{\langle c,d\rangle | T_t(a,c,d)\} \cup \{\langle c,0\rangle | E(a,c)\}$ with each state a, where c is the class number in E of a, and the d's are the class numbers of states reachable from a by transition t.

Let $Sig(a)$ be the signature $\{\langle c,d\rangle | T_t(a,c,d)\}$ associated with state a

$newmap(s) = j \in \mathbb{N}^+$, a function that associates a unique positive integer (a new class number) with each different signature s, so that $\forall s_1, s_2 \in \{Sig(a) | a \in domain(E)\} : newmap(s_1) = newmap(s_2) \iff s_1 = s_2$

$E'(a,k) \triangleq k = newmap(Sig(a))$ a new partition that associates each state a with its new class number

Now define the function $RefineH$ as: $RefineH_1 \circ RefineH_2 \circ \ldots$, composing $RefineH_t$ for all transition labels t

Finally, starting with an initial partition based on state labels, $E_0(s,k) = (s$ has the kth state label), Calculate the closure of $RefineH$ on E_0, yielding $E_{n_{max}} = RefineH(E_{n_{max}})$, where $E_{n+1} = RefineH(E_n)$.

$E_{n_{max}}$ is the equivalence relation for the relational coarsest partition of the given labeled transition system. This is calculated using the following variation on algorithm 1.2. It uses a helper function, *SigRenum*, to renumber the partition classes.

Algorithm 7:

```
MDD HybridClosure( ℕ N_transition_labels, MDD Q_[], MDD S ) is          • (Calculate E_n_max)
  local MDD E, MDD E_old, MDD W, MDD T_partial[], MDD T_[]
 1  E ← DC_2(S, {1})                  • E(a,1) for all a, (put all states it the only class (1) of the partion)
 2  repeat                            • E ← RefineH*( E ) until E = RefineH( E )
 3    E_old ← E
 4    for t ∈ [0, N_transition_labels) loop
 5      W ← DC_3(E, {0})              • has the same range as E
 6      T_partial[t] ← proj_∨2(DC_4(DC_3(Q_t, [0,|S|]), [0,|S|]) ∩ DC_4(DC_2(E,S), [0,|S|]) ∩ DC_1(DC_2(E, [0,|S|]), S))
      • T_partial[t](a,c,d) = ⋁ b : (Q_t(a,b) ∧ E(a,c) ∧ E(b,d))
 7      T_[t] ← T_partial[t] ∪ W      • make the signature relation total by including range of E
 8      E ← SigRenum( T_[t] )         • renumber partition classes
 9    end loop
10  until E = E_old
11  return E                          • E_n_max
```

Algorithm 7, Closure of hybrid partition refinement, with forwarding.

Although this algorithm appears very similar to algorithm 1.2, it is optimized to support non-interleaved ordering for representation of the equivalence relation, while the transition relation Q_t is represented as an interleaved MDD. The interleaving intrinsic to Q_t is eliminated in line 6, where the variables and levels corresponding to parameter b of Q_t are eliminated by projection. As only the parameters a and b of Q_t were interleaved, no interleaving remains. The explanation of the signature relation of Algorithm 1 also applies here to some extent. For this $\mathcal{T}_{partial[t]}$ constructed in line 6, the meaning is similar to the meaning of $\mathcal{T}_t$ from Algorithm 1, except numbers are used to represent partitions classes in $\mathcal{E}$. $\mathcal{T}_{partial[t]}$ (a, b) means that a has a transition to the class containing b. There is one complication. The construction of $\mathcal{T}_{partial[t]}$ gives it the same domain as Q_t, which may not be the entire state space S. Also, this algorithm does not operate by removing pairs from E as does Algorithm 1. This algorithm operates by replacement of E. As it would be unacceptable to lose members of the state space from the domain of E, we use an extra MDD $\mathcal{W}$ to ensure that members are not lost. Line 5 constructs $\mathcal{W}$ with the same domain as $\mathcal{E}$, using a distinct unused partition class number as the only element of the range. This enters into the total signature relation $\mathcal{T}_t$ in line 7. The call to *SigRenum* on line 8 finally assigns a new class number to each equivalence class, as refined using the total signature relation $\mathcal{T}_t$

5.9 Unified calculation of: $DC_4(DC_3(Q,[0,|S|]),[0,|S|])\cap DC_4(DC_2(E,S),[0,|S|])\cap DC_1(DC_2(E,[0,|S|]),S)$

Given decision diagrams representing a transition relation $Q \subseteq \hat{S} \times \hat{S}$, and an equivalence relation $E \subseteq S \times [1,N]$, where $N = |S|$, produce a decision diagram representing the unquantified composition $t \subseteq S \times S \times [1,N] \times [1,N] = DC_4(DC_3(Q,[0,|S|]),[0,|S|]) \cap DC_4(DC_2(E,S),[0,|S|]) \cap DC_1(DC_2(E,[0,|S|]),S))$ of Q and E, so that:

$\forall a,b \in \hat{S}, c,d \in [1,N] : t(a,b,c,d)$ iff $Q(a,b) \wedge E(a,c) \wedge E(b,d)$

I assume that the variable levels in t and Q corresponding to parameters a and b occur in the same ordering, and also that the variable levels in t and E (the first occurrence) corresponding to parameters a and c occur in the same ordering. Also, of course, the variable levels in t and E (the second occurrence) corresponding to parameters b and d occur in the same ordering.

Assume that a diagram representing $\hat{S}$ or S has K levels, a diagram representing $[1,N]$ has $M = \lceil \log_2(N+1) \rceil$ levels, a diagram representing E has $K+M$ levels, a diagram representing Q has $2K$ levels, and a diagram representing t has $2K+2M$ levels.

We produce t as follows: Let $t \leftarrow$ *UcompH*($2K+2M$, Q, E, E),

where *UcompH* is computed as in:

Algorithm 8:

```
MDD UcompH( ℕ L, MDD Q, MDD E1, MDD E2 ) (memoized function) is
  local  MDD  R
   1 if UcompH( L, Q, E1, E2 ) is found in cache, return UcompH( L, Q, E1, E2 ) from cache
   2 if level L of the output is leaves, then                    • Q, E1 and E2 will also be leaves
   3   R ← Q ∩ E1 ∩ E2, using leaf rules
   4 else if level L of the output corresponds to parameter a then   • DC1(DC2(E)) has a don't care at this level
   5   if Q = ∅ ∨ E1 = ∅ ∨ (Q and E1 have no children with same index) then R ← ∅, else:
   6     create a new MDD node R
   7     for each child q of Q and child e of E1, having the same index, loop   • use only a where Q(a,*) and E(a,*)
   8       place a corresponding child UcompH( L − 1, q, e, E2 ) into R
   9     end loop
  10   end if
  11 else if level L of the output corresponds to parameter b then   • DC4(DC2(E)) has a don't care at this level
  12   if Q = ∅ ∨ E2 = ∅ ∨ (Q and E2 have no children with same index) then R ← ∅, else:
  13     create a new MDD node R
  14     for each child q of Q and child e of E2, having the same index, loop   • use only b where Q(*,b) and E(b,*)
  15       place a corresponding child UcompH( L − 1, q, E1, e ) into R
  16     end loop
  17   end if
  18 else if level L of the output corresponds to parameter c then   • DC4(DC3(Q)), DC1(DC2(E)) have don't cares
  19   if E1 = ∅ then R ← ∅, else:
  20     create a new MDD node R
  21     for each child e of E1 loop
  22       place a corresponding child UcompH( L − 1, Q, e, E2 ) into R
  23     end loop
  24   end if
  25 else (level L of the output corresponds to parameter d)   • DC4(DC3(Q)), DC4(DC2(E)) have don't cares
  26   if E2 = ∅ then R ← ∅, else:
  27     create a new MDD node R
  28     for each child e of E2 loop
  29       place a corresponding child UcompH( L − 1, Q, E1, e ) into R
  30     end loop
  31   end if
  32 end if
  33 R ← unique( R )
  34 enter R = UcompH( L, Q, E1, E2 ) into cache
  35 return R
```

Algorithm 8, an unquantified composition, using E two ways

As with Algorithm 6 and Algorithm 4, *UcompH* recursively constructs its output, constructing each level by cloning corresponding parts of input MDDs. In this case, there are four parameters involved, necessitating the four cases (lines 5-10 for parameter a, lines 12-17 for b, lines 19-24 for c, and lines 26-31for d). Otherwise, the same principles generally apply.

5.10 Numbering of equivalence classes of a signature relation

Given a decision diagram representing an signature relation $E \subseteq S \times K$, assign a unique partition number n_k to each signature k of K in the range of E, and produce a partition relation E' such that $E'(s, n_k) = E(s, k)$.

Conveniently, we can use the canonicity of decision diagrams to our advantage. Each unique signature value k in K will be represented by a unique DD. Consequently one need only traverse the diagram, representing E, and replace each new member of K encountered, with a new integer, obtained by incrementing a global counter. We use the built-in caching functions of the SMART MDD library, to memoize the function implementing our algorithm. This ensures that each occurrence of the same signature is replaced by the same unique partition number,

The function will be performed as follows: *init_SigRenum*(); $E' \leftarrow$ *SigRenum*(E), where *init_SigRenum*() and *SigRenum* are defined as follows:

Algorithm 9:

```
init_SigRenum() is
  global  ℕ  counter
   1 clear cache for SigRenum( MDD ℰ )
   2 counter ← 0
```

```
MDD SigRenum( MDD ℰ ) (memoized function) is
  global  ℕ  counter
  local  MDD  ℛ
   1 if SigRenum( ℰ ) is found in cache, return SigRenum( ℰ ) from cache
   2 ℛ ← a new empty MDD node
   3 if ℰ is at the level of the signature in this DD, then
   4   counter ← counter + 1;                    • if we got here, the signature is new, assign unique number
   5      into ℛ insert child BDD representing value counter
   6 else                                  • not at signature level, just duplicate node, with function applied recursively
   7   for each child e of ℰ loop                          • Use bits of counter to construct a narrow BDD
   8     let v be the value at this level for e within ℰ in:
   9       into ℛ insert child SigRenum( e ), with value v
  10   end loop
  11 end if
  12 ℛ ← unique( ℛ )
  13 enter ℛ = SigRenum( ℰ ) into cache
  14 return ℛ
```

Algorithm 9, renumbering of signatures

As with many other algorithms, the algorithm *SigRenum* recursively copies its input MDD to its output while doing depth-first-traversal. This can easily be seen in lines 7-10. This algorithm expects signatures to occur at some known level of the MDD. In the output, this algorithm replaces each different signature with a unique partition class number. Each new class number is produced by incrementing a counter on line 4. The number is represented by a narrow (where each node has exactly one child, except the leaf) BDD. The BDD is constructed by using the bits from the binary representation of the number as the values of variables at the levels of the BDD.

6 Design

The software implementation of this work is implemented as a unit of code within the latest revision of the SMART verification tool. Its activation is prompted by a `num_eqclass()` command in a model within a SMARTsource file.

The functionality provided to SMART by the software implementation is as follows. SMART calls the function:

```
bigint ComputeNumEQClass(state_model *mdl);
```

passing a `state_model *mdl` , which is a representation of a state transition system. This function, after calculating the relational coarsest partition for the given model, calculates the number of partition elements in the coarsest refinement, and returns that number, as a `bigint`, to SMART. A `bigint` is a data type capable of storing finite integers that may require very many digits for their representation.

1. The `ComputeNumEQClass` function is a glue function, which invokes an internal `ComputeNumEQClass` function.

   The internal `ComputeNumEQClass` function extracts the state space and the transition relations from its input, then, to produce the result, calls the following other internal functions:

2. `Mdd *BooleanInterleavedLumping( Mdd * * Qarray, int NQ, Mdd *S, int L );` calculates the relational coarsest partition, using the interleaved representation for the partition relation, given the array `Qarray` of interleaved MDDs representing the transition relations, the number `NQ` of transition relations, the MDD `S` for the state space, and the number `L` of levels in the MDD `S` .

3. `Mdd *BooleanHybridLumping( Mdd * * Qarray, int NQ, Mdd *S, int L );` calculates the relational coarsest partition, using the non-interleaved representation for the partition relation, given the array `Qarray` of interleaved MDDs representing the transition relations, the number `NQ` of transition relations, the MDD `S` for the state space, and the number `L` of levels in the MDD `S` .

4. `bigint CountEQClasses( Mdd * E, Mdd * S )` calculates the number of partition elements, given the interleaved MDD `E`, representing the partition, and the MDD `S`, representing the state space.

5. `Mdd *sigrenumQ( Mdd *E, int level, int & count )` calculates the number of partition elements, given the non-interleaved MDD `E`, representing the partition, and the MDD level `level`, indicating which levels of `E` store signatures.

   The other internal functions operate as follows:

6. The `BooleanInterleavedLumping` function performs the *RefineClosure* algorithm, as shown in Algorithm 1.2. It calls `InsertDontCaresQQ` to construct the initial partition ($S \times S$). It calls `RelationalComposeInterleavedQQ` to perform the composition calculation on line 5 of Algorithm 1.2. It calls `NegEquivClassInterleavedQQ` to perform the class construction calculation on line 6 of Algorithm 1.2.

7. The `BooleanHybridLumping` function performs the *HybridClosure* algorithm, as shown in Algorithm 7. It calls `sigrenumQ` to construct the initial partition ($DC_2(\mathcal{S}, \{1\})$). It calls `InsertDontCaresQQ` to construct $\mathcal{W}$, as described on line 5 of Algorithm 7. It calls the `GenericComposeQQ` function followed by `ProjectUnionQQ` to perform the composition calculations on line 6 of Algorithm 7. It calls `sigrenumQ` to perform the class renumbering calculation on line 8 of Algorithm 7.

8. The `CountEQClasses` function performs the calculation: $N_E \leftarrow mag(\ S \setminus proj_{\vee 2}(\ selectNonMin(E)\ )\ )$. It calls the `selectGT` function to perform the *selectNonMin* algorithm. It also calls the `ProjectUnionQQ` function to perform the projection ($proj_{\vee 2}$).

9. The `Mdd * RelationalComposeInterleavedQQ` function accepts the following parameters:

   (

   `Mdd *left,` a MDD representation of a first relation $\mathcal{Q}$

   `bool *Lleft,` a selection of surviving variables

   `Mdd *Uleft,` a MDD for the set of possible states of the surviving variables $\mathcal{S}_{\mathcal{Q}}$

   `Mdd *right,` a MDD representation of a second relation $\mathcal{E}$

`bool *Lright,` a selection of surviving variables from the second relation

`Mdd *Uright` a MDD for the set of possible states of the surviving variables from the second relation $\mathcal{S}_\mathcal{E}$

`);` and returns a MDD representing the composition $\mathcal{T} \subseteq \mathcal{S}_\mathcal{Q} \times \mathcal{S}_\mathcal{E} = \mathcal{Q} \circ \mathcal{E}^{-1}$,

such that $\mathcal{T}(q, e) = \bigvee c : (\mathcal{Q}(q, c) \wedge \mathcal{E}^{-1}(c, e)) = \bigvee c : (\mathcal{Q}(q, c) \wedge \mathcal{E}(e, c))$.

It performs this composition as: $\mathcal{T} \leftarrow proj_{\vee 3}((DC_2(\mathcal{Q}, \mathcal{S}_\mathcal{E})) \cap (DC_1(\mathcal{E}, \mathcal{S}_\mathcal{Q})))$, and so can be used to implement the pseudo-code on line 5 of *RefineClosure* in Algorithm 1.2. It calls `GenericComposeQQ` to compute the MDD for $(DC_2(\mathcal{Q}, \mathcal{S}_\mathcal{E})) \cap (DC_1(\mathcal{E}, \mathcal{S}_\mathcal{Q}))$. It also calls `ProjectUnionQQ` to calculate the projection operation $(proj_{\vee 3})$.

10. The `Mdd *NegEquivClassInterleavedQQ` function accepts the following parameters:

    `(`

    `Mdd *T,` a MDD representing a signature relation $\mathcal{T}$. The set $\{b|\mathcal{T}(a, b)\}$ is the signature of a

    `bool * L,` a selection of variables representing the signature part of the relation $\mathcal{T}$

    `Mdd *U );` a MDD for $\mathcal{S}$ (the state space) the set of objects that have signatures in $\mathcal{T}$

    It returns an MDD representing the partition of those $\mathcal{S}$ into classes of members having the same signature. The returned MDD encodes the complement of the equivalence relation: $\mathcal{E}(s_1, s_2) \in \mathcal{S} \times \mathcal{S} = \bigwedge t : (\mathcal{T}(a, t) = \mathcal{T}(b, t))$. This output is calculated as: $\overline{\Delta\mathcal{E}} \leftarrow proj_{\vee 3}(DC_2(\mathcal{T}, \mathcal{S}) \cup DC_1(\mathcal{T}, \mathcal{S}))$, and so may be used to implement the pseudo-code on line 6 of *RefineClosure* in Algorithm 1.2. It calls `InsertDontCaresQQ` to compute the MDDs for the expressions $DC_2(\mathcal{T}, \mathcal{S})$ and $DC_1(\mathcal{T}, \mathcal{S})$. It also calls `ProjectUnionQQ` to calculate the projection operation $(proj_{\vee 3})$.

11. The function `Mdd *InsertDontCaresQQ` accepts the following parameters:

    `( int L,` the height of (number of variables in) the MDD to be constructed.

    `Mdd *d,` the input MDD, for the set D of the values of the original variables

    `bool * inserts,` a selection of variables in the output MDD which will be don't-care variables

    `Mdd * U );` an MDD for the universe, from which values of don't care variables may be drawn

    It returns an MDD for a set D', where $D'(\ldots$ D-variables and U-variables $\ldots) = D(\ldots$ D-variables $\ldots) \wedge U(\ldots$ U-variables $\ldots)$. The result is calculated using the algorithm for DC, from the algorithms section, and so can be used to implement any of the forms of DC_1 and DC_2 found in the various algorithm pseudo-codes.

12. The `Mdd * ProjectUnionQQ` function accepts the following parameters:

    `(`

    `Mdd * arg,` a MDD for the set/relation F to be projected

    `bool * projectible );` a selection of levels of the variables to be eliminated by disjunction

    It returns a MDD for the projection F' of the relation F, such that $F'(\ldots$ surviving variables $\ldots) = \bigvee$ projectible variables : $F(\ldots$ surviving variables and projectible variables $\ldots)$. It uses the *projectUnion* algorithm previously given, and so can be used to implement all the various forms of $proj_\vee$ found in the above algorithms. It calls the `OperateUnionQQ` function to implement the *operateUnion* function found on line 11 of the *projectUnion* algorithm.

13. The `Mdd * OperateUnionQQ` function accepts an argument:

    `( Mdd * arg );` an MDD F

The function returns a MDD for the union of all children of the top node of F. The union is calculated according to the algorithm for *operateUnion*, given above, and is used to implement line 11 of the *projectUnion* algorithm.

14. The `Mdd * selectGT` function accepts the parameter:

    `( Mdd * Eb );` a MDD, representing a set, E_b, of pairs of states that is an equivalence class

    and returns a MDD for a set E' of pairs such that $E'(b,c) = b \not\leq c \wedge E_b(b,c)$ (using lexicographic ordering). This result is calculated using the *selectNonMin* algorithm, previously given, and is used by the `CountEQClasses` function to determine the number of classes in an equivalence class.

15. The `Mdd *GenericComposeQQ` function accepts the parameters:

    `(`

    `Mdd *operand1,` a first operand

    `Mdd *operand0,` a second operand

    `Mdd *range,` a third operand, normally used to limit the function output

    `int N );` the number of levels for the output MDD

    and other parameters, encoding an operation description.

    This function performs a composition operation, among the three operands, producing a composed MDD output having `N` levels. This composition function evaluates compositions such as $(DC_2(Q,S)) \cap (DC_1(E,S))$, and $DC_4(DC_3(Q,[0,|S|]),[0,|S|]) \cap DC_4(DC_2(E,S),[0,|S|]) \cap DC_1(DC_2(E,[0,|S|]),S)$, in a recursive manner without constructing the MDDs representing any of the sub-expressions. Hence, it is able to efficiently implement the *UcompL* method of Algorithm 6, and the *UcompH* method of Algorithm 8, and is used for those purposes by the `RelationalComposeInterleavedQQ` function and the `BooleanHybridLumping` functions.

16. The `Mdd *sigrenumQ` function accepts the following parameters: `( MDDL::MddNode *E,` A non-interleaved MDD representing a signature relation `int level,` The top level in E at (and below) which the signatures are represented `int & count );` A reference to the global counter as described in Algorithm 9.

    This function returns a MDD analogous to its input `E`, with each different signature (at level `level`) replaced by a unique class number, starting at 1. This replacement of signatures by unique numbers is performed according to the *SigRenum* method of Algorithm 9. The global counter `count` will contain the number of signatures/classes found in `E`, upon return from this function.

Note: Some omissions and contractions occur in the above, to simplify the presentation.

7 Project History

Motivated by the need for more efficient lumping algorithms, we surveyed the relevant literature. Guided by the advisor's idea to use interleaved MDDs to represent partitions, we soon devised Algorithm 1, for bisimulation, and a variant, Algorithm X, for lumping. Imminency of deadlines forced a limitation of the scope of this project. As Algorithm X promises to require more effort, to implement AAMDDs or to convert EV*MDDs to EV$^+$MDDs, we chose to first implement Algorithm 1.2, to gauge the feasibility of using interleaved MDDs to represent partitions. Our first implementation of *RefineClosure* used interleaved representation for all relations. After coding

RefineClosure, we surveyed the literature relevant to this type of bisimulation, and surprisingly found that Algorithm 1 had been discovered by 1992 by Amar Bouali and Robert De Simone[1]. Amar Bouali and Robert De Simone also provide performance comparison, between use of interleaved BDDs, and use of non-interleaved BDDs. We then chose to compare with the performance of Algorithm H, which uses interleaved MDDs for the transition relations, and non-interleaved MDDs for the equivalence relation representing the partition of the state space. The equivalence relation is constructed in a manner similar to that used in the lumping algorithm described by Derisavi [5]. This is intended to provide a comparison between the use of interleaved and non-interleaved MDDs, that applies specifically to the equivalence relation. We also constructed some additional parametric sets of models to compare these bisimulation algorithms. The results we obtained are as follows:

8 Results

We obtained the following results, running both the fully implicit algorithm and the hybrid algorithm on a set of parametric models from two classes. The short model is a simple Petri net with 6 places parameterized in the number of tokens in a particular place in the start state. The tall model is a variable simple sized Petri net parameterized in number of places, always starting with one token in a particular place. In these tables, N denotes the parameter value, $|S|$ is the number states, "classes" is the number of equivalence classes in the final partition, "nodes max" is the maximum number of MDD nodes used during the calculation, "output nodes" is the number of nodes used to store the final partition MDD, "count" is the number of iterations required to converge, and "cpu" is the algorithm execution time in seconds.

8.1 Results on bisimulation of short model

8.1.1 Hybrid Algorithm

N	$\|S\|$	classes	nodes max	output nodes	count	cpu
1	6	5	606	38	3	0.005051
2	20	15	2286	104	3	0.015124
3	50	35	6913	232	4	0.049227
4	105	70	11945	462	4	0.145402
5	196	126	16015	854	5	0.43089
6	336	210	25027	1466	6	1.07963
7	540	330	31490	2415	7	2.32819
8	825	495	45321	3370	8	4.73165
9	1210	715	65425	5158	9	9.40929
10	1716	1001	91360	6820	10	15.9901
11	2366	1365	134295	9963	11	30.8077
12	3185	1820	177807	12616	12	49.2111
13	4200	2380	252386	17934	13	87.9802

8.1.2 Fully Implicit Algorithm

N	$\|S\|$	classes	nodes max	output nodes	count	cpu
1	6	5	1268	43	3	0.010727
2	20	15	8870	100	3	0.083595
3	50	35	21334	189	4	0.95391
4	105	70	59776	316	4	5.103
5	196	126	170998	487	5	32.5523
6	336	210	387343	708	6	179.014
7	540	330	653046	985	7	883.247
8	825	495	1322487	1324	8	3747.09
9	1210	715	2527232	1731	9	13440

8.2 Results on bisimulation of tall model

8.2.1 Hybrid Algorithm

N	$\|S\|$	classes	nodes max	output nodes	count	cpu
1	3	3	217	17	2	0.001857
2	6	5	526	38	2	0.003994
3	11	7	1200	63	4	0.009415
4	18	9	2341	104	6	0.019422
5	27	11	3852	145	8	0.037592
6	38	13	5955	207	10	0.060027
7	51	15	8460	266	12	0.090472
8	66	17	11590	349	14	0.1646
9	83	19	12172	424	16	0.196967
10	102	21	12737	507	18	0.253873
11	123	23	13690	598	20	0.357343
12	146	25	14596	722	22	0.437878
13	171	27	15629	831	24	0.58964

8.2.2 Fully Implicit Algorithm

N	$\|S\|$	classes	nodes max	output nodes	count	cpu
1	3	3	291	16	2	0.002874
2	6	5	1012	43	2	0.007588
3	11	7	4271	99	4	0.035115
4	18	9	12671	187	6	0.101841
5	27	11	17225	307	8	0.362121
6	38	13	25421	459	10	0.869437
7	51	15	41643	643	12	2.95264
8	66	17	64886	859	14	4.63575
9	83	19	86394	1107	16	9.52985
10	102	21	124779	1387	18	18.877
11	123	23	174345	1699	20	34.7302
12	146	25	236927	2043	22	58.943
13	171	27	314335	2419	24	97.8769

Inspection of the results shows that, by most measures, the fully implicit algorithm did not outperform the hybrid model. The exception to this was in the size of the output for the short model. In this one case we see that the interleaved ordering provides some improvement over the non-interleaved ordering, for the storage of the final partition MDD. For clarity, that set of data is displayed in graphical form as Figure 11.

9 Conclusions

Although the present results appear to be inauspicious for the use of fully interleaved representation of partitions, it should be noted that these results cannot be considered conclusive. The limitation in scope of this project did not permit the consideration of all the obvious possibilities for optimization. The evaluation of the expression $DC_2(\mathcal{T}_t, \mathcal{S}) \cup DC_1(\mathcal{T}_t, \mathcal{S})$, in the *RefineClosure* algorithm is performed as defined ($F \cup G \triangleq F \setminus G \cup G \setminus F$), resulting in several (potentially large) intermediate data structures. This expression could be evaluated in an integrated manner, avoiding the production, storage, and processing of those intermediate data structures. The only conclusion that can be drawn at this time is that more possibilities for optimization should be explored.

10 Future Work

We expect to integrate the evaluation of $DC_2(\mathcal{T}_t, \mathcal{S}) \cup DC_1(\mathcal{T}_t, \mathcal{S})$ of *RefineClosure* into a single algorithm, as a possible improvement to the present work, among other enhancements.

We expect to extend the use of the interleaved representation of partitions to Markov Lumping (see Algorithm X in appendix X). Additionally, similarly to [8], we expect to use the notion of *minimum distance*, although [8] used *rank*, to provide additional acceleration for Markov Lumping. We expect that the use of minimum distance, instead of rank, will produce an improvement in execution time, since minimum distance has been shown [3] to be efficiently computable using *saturation* methods. Additionally, minimum distance, unlike rank, is well defined

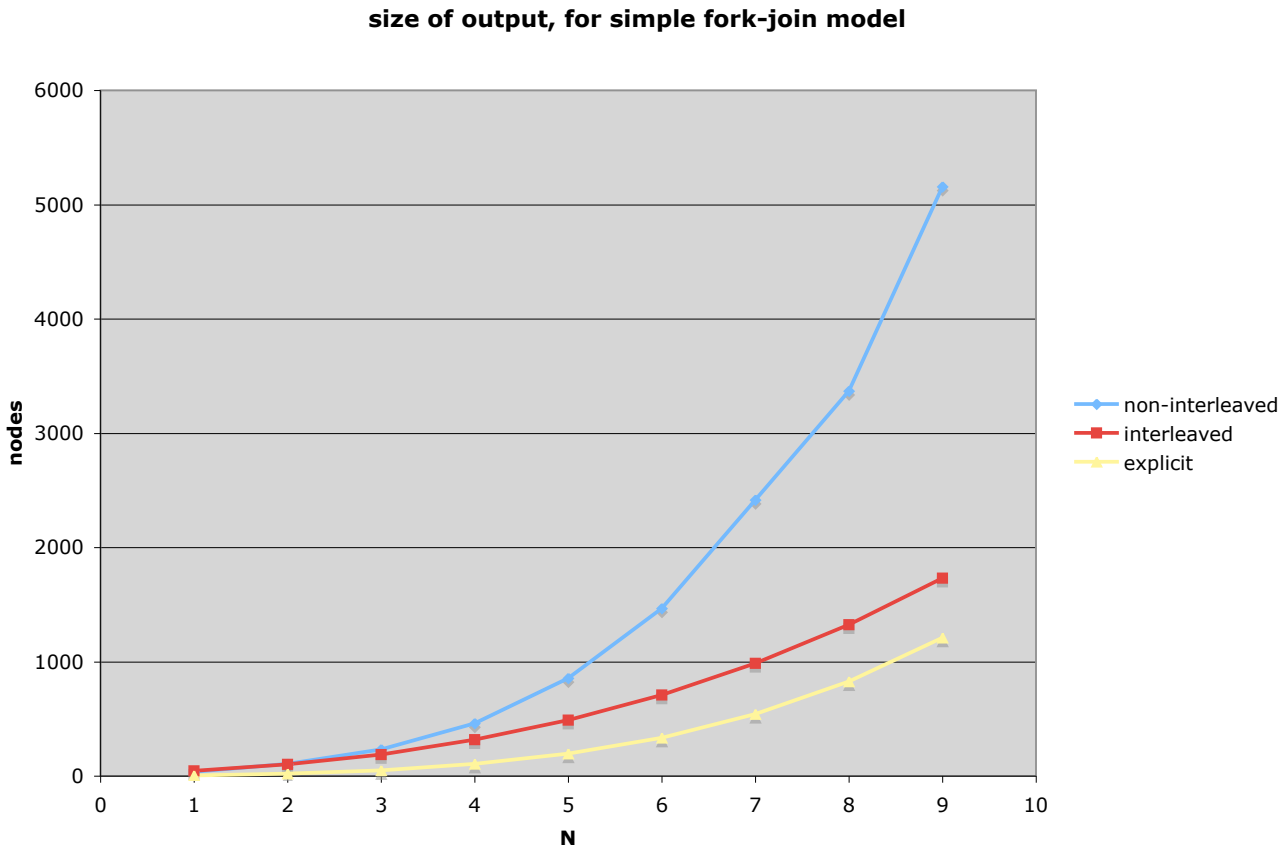

Figure 11: Number of nodes in output MDD, non-interleaved vs. interleaved vs. explicit

in the presence of cycles.

Also, we would like to explore the direct use of saturation methods to compute the complement of the maximum bisimulation. The complement of the bisimulation is the space of pairs of distinguishable states. Some pairs are initially known to be distinguishable due to different markings, or due to different transition enablements. The transition relations (and their inverses) can be used to infer new pairs of distinguishable states from existing pairs. This situation is analogous to the search of a state space, for which saturation is quite efficient.

Future updates of this work may be found at:

`http://www.cs.ucr.edu/~mummem/{bisimulation,lumping,MSproject}` .

11 Related work on Markov Lumping

11.1 Bisimulation algorithms for stochastic process algebras and their bdd-based implementation [10]

This article by Hermanns and Siegle explains how to use BDD's and interleaved ordering for the purpose of solving Markov chains.

To find a way to efficiently store rate information in association with BDDs, the authors define "decision nodes" of a BDD. They show that a path through a BDD is uniquely defined by the sequence of decision nodes on that path.

"A decision node is a non-terminal BDD node whose successor nodes are both different from the terminal false-node."

They then define a DNBDD (Decision Node BDD) that associates 2^k rates with each sequence of decision nodes on a path through the BDD, where k is the number of "don't care" variables on the path. To provide efficient access to the stored rates, they are placed in a "rate tree" parallel to the BDD. They do not clearly define notion of rate trees.

This structure saves some space compared to the most naive approach by effectively factoring out "don't care" nodes. It should be noted, however, that 2^n rates are stored in the structure, n being the number of variables.

11.2 Optimal state-space lumping in Markov chains [6]

This paper by Derisavi, Hermanns, and Sanders, points out that the $O(m(log(n)))$ bound, for lumping Markov chains, claimed in some other papers (on explicit state space lumping), usually by reference to [14], is not actually proven in those papers. The $O(m(log(n)))$ bound, proven in [14], is for the non-stochastic case, while the other papers discuss the stochastic case. This bound may be exceeded, in the stochastic case, as follows: When splitting some set B using splitter S, many members of B may have the same aggregate rate for edges to S, hence they will remain together after splitting. It is necessary to identify those members with the same aggregate rate, by using some associative data structure. The usual data structures, such as 2-3 trees, will require $O(|B|log|B|)$ time to identify those cases. This additional factor of $log|B|$ during splitting increases the overall bound to $O(m(log(n))^2)$. This extra factor of time usage may occur in cases where splitting does not yield many products.

As a worst-case example, consider the case where every splitting operation produces two new equal sized members from each existing partition member, and the lumped result is the same as the result without lumping. Suppose additionally that $m \in O(n)$, in the main problem, and in sub-problems, so that $O(m(log(n))) = O(n(log(n)))$. In this case, the first split produces 2 members, each of size $n/2$, at a cost of $O(nlog(n))$. This cost is $O(n(log(n)))$, instead of $O(n)$, because of the use of some typical associative data structure to sort $O(n)$ members by their aggregate rates. The problem is now reduced to two sub-problems, each of size $n/2$. In this case, solving the resulting recurrence reveals the time overall complexity is $O(n(log(n))^2)$.

The contribution of this paper is to apply splay trees to this purpose. Due to the static optimality property of splay trees, some savings is obtained in the case where there are multiple members of B with the same aggregate rate. They show that the savings are sufficient to bring the overall bound back to $O(m(log(n)))$.

In the above example, each splay tree operation will usually occupy constant time, instead of O($log(n)$) time, since there are only two different aggregate rates.

I would like to point out that a slightly modified merge-sort also has sufficient savings in this case. If the merge phase of a merge-sort is modified to consolidate items with the same key, the savings will also be sufficient to achieve the same bound. Applying this to the above example, each merge operation will only take constant time, as every list will be at most length two, since there are only two key values.

11.3 Lumping matrix diagram representations of Markov models [7]

This article by Derisavi, Kemper, and Sanders explains an efficient, but not optimal, application of *matrix diagrams* (MDs) to the lumping problem. A matrix diagram is a DD-like representation of a matrix. Each vertex of an MD represents a matrix. Each edge of an MD also represents a matrix. The matrix represented by a vertex is the sum of the matrices represented by its outgoing edges. Each edge also is decorated with a matrix r. The matrix represented by the edge is the tensor product of r with the matrix represented by the destination vertex. An MD has uniform depth, as with DDs. The leaves represent scalars (usually only one shared leaf, representing 1.0) At each level of the MD, the edge decorations r have identical dimensions; consequently, all the matrices represented at a given level also have identical dimensions.

State transition rate matrices are represented by MDs, usually using an encoding similar to variable interleaving. Each level usually encodes a few related variables in both the starting and ending state. The paper shows how to do lumping at each level separately from the other levels. After each level is lumped and the results composited, the output MD may involve considerably fewer macro-states than the input MD. Optimality, however, is not guaranteed, as it is with many other lumping methods. Experiments have shown the lumping method to be very fast compared with other methods, however the output is usually of lower quality.

It seams to me that this type of lumping would be useful for pre-processing the input to an optimal algorithm. It would be very efficient, and the optimal algorithm might run faster because its input is already partly lumped.

11.4 A symbolic algorithm for optimal Markov chain lumping [4]

This paper by Derisavi introduces a novel technique for the symbolic representation of partitions, and a lumping algorithm to use this representation. His method represents a partition of n blocks using O($log(n)$) sets, represented as BDDs. A partition of a set S, where there are $n = 2^k$ blocks, is represented as the family of sets: $\{P_0, \ldots, P_{k-1}, S\}$. A member c of block C is a member of P_j iff the j-th bit of C's index is 1. In this representation, any block C can be reconstructed as follows:

$$C = \bigcap_{j \in [0,k-1]} \left\{ \begin{array}{ll} (P_j) & \text{when} j\text{-th bit of } C\text{'s index is 1} \\ (S - P_j) & \text{when} j\text{-th bit of } C\text{'s index is 0} \end{array} \right\}$$

The set of members of a given block can be extracted from this representation using O(k) = O($log(n)$) set operations. It also takes O($log(n)$) set operations to insert an element(s) into or remove an element(s) from a block. Additionally, an algorithm is given for traversing (sequentially extracting) all n blocks using O(n) set operations, using a stack of O($log(n)$) sets.

Given these properties of their data structure, the lumping algorithm starts with an initial partition, with the

blocks numbered contiguously, starting at 0. Each iteration uses one block to split all the other blocks, taking the splitters sequentially, starting at block 0. Each new block created by splitting is given the next sequential index after the existing blocks. The aggregate rates are computed symbolically.

Additionally, it is shown how to efficiently identify the case where a block is (or many contiguous blocks are) stable, with respect to a splitter, allowing the processing of those blocks to be skipped. A block C is stable under splitting by block B iff $C \cap B' = \emptyset$, where B' is the set of states having non-zero transition rates to at least one element of B. Using the definition of C above, we have:

$$C \cap B' = \bigcap_{j \in [0,k-1]} \left\{ \begin{array}{ll} (P_j) \cap B' & \text{when} j\text{-th bit of } C\text{'s index is 1} \\ (S - P_j) \cap B' & \text{when} j\text{-th bit of } C\text{'s index is 0} \end{array} \right\}$$

The O($log(n)$) values $(P_j) \cap B'$ and $(S - P_j) \cap B'$ can be pre-computed at the beginning of a phase where blocks are to be split by splitter B. Similarly to the computation of C, the values of $C \cap B'$ can be sequentially extracted in a linear number of set operations. In the course of computing $C \cap B'$ using the above formula, one computes the partial intersection:

$$C_{[0,l-1]} \cap B' = \bigcap_{j \in [0,l-1]} \left\{ \begin{array}{ll} (P_j) \cap B' & \text{when} j\text{-th bit of } C\text{'s index is 1} \\ (S - P_j) \cap B' & \text{when} j\text{-th bit of } C\text{'s index is 0} \end{array} \right\}$$

for each $l < k$, using the prefix consisting of bits $0 \ldots l-1$ of the index of block C. If one of these partial intersections is empty, then any block, C', whose index is an extension of the same prefix, has the following property:

$C' \cap B' = \emptyset$

Consequently all such C' are stable under splitting by B, and their processing may be skipped.

11.5 Signature-based symbolic algorithms for optimal Markov chain lumping [5]

In this article by Derisavi, MTBDDs are used to represent transition rate matrices and partitions. Interleaved ordering is used for state variables, and an additional variable is added to indicate a block number in a partition. When partitions are represented, one of the (interleaved) state variables is taken to be a don't care. When doing computations involving rate (Q) matrices, they actually represent the diagonal and non-diagonal elements in separate MTBDDs, to avoid an explosion of the MTBDD due to representing all of the diagonal elements.

Since each diagonal element is a linear function of the sum of the other elements in the same row, the diagonal elements are likely to be unique. At any given level of a canonical DD, the number of elements at that level is the number of unique values at that level. Consequently, at the level of values in the MTBDD that represents Q, there would likely be as many values (and elements) as there are states in the Markov chain. Such an explosion in the size of the data structures eliminates many advantages of using symbolic methods. The diagonal elements are instead represented in a way that takes advantage of the symmetry of the diagonal element matrix, and are effectively calculated when needed.

His main algorithm builds on other work with algorithms that split blocks with respect to all available splitter blocks in a single large step. He shows how to use CUDD[16] operations to symbolically compute the aggregate rates of elements to all splitters. Although he mention the consideration of interleaved state variables, it appears that they represent partitions and signatures in a non-interleaved manner. It appears that, at this stage, part of

their data structure will have a vertex corresponding to each new block (explaining a later observation). This is because the partition index is stored as a terminal node, and a signature is represented with its variables close to the leaves, below the level of state variables. The number of nodes at a given level is the number of unique trees stored at that level. In this case that corresponds to the number of signatures (partition blocks).

Because of the particular variable ordering of his BDDs, this algorithm can simply substitute a new block index at all the unique nodes of a certain level, to construct the new partition. As his algorithm is, at that stage, it ignores current block boundaries, constructing the new partition strictly on the basis of the set of aggregate rates ("signature"). He repairs this situation by including the current block number, by an arithmetic encoding, into the "signature", so that the new partition will be a refinement of the previous partition.

Experimentally, He observes that the algorithm is faster then the previous algorithm [4], but requires more space.

12 Appendices

12.1 Appendix X

This lumping algorithm is almost identical to bisimulation Algorithm 1, except that three operations are replaced, and an EV$^+$MDD or an AADD is used for the $\mathcal{Q}$ parameter.

The following additional definitions are required:

$DC_2(F,G)(x,a,y) \triangleq F(x,y)$ whenever G(a) inserts don't-care variable in position 2 (extended for EV$^+$MDD F)

$proj_{\Sigma 3}(F)(x,y) \triangleq \Sigma_a F(x,y,a)$ project third variable by summation (EV$^+$MDD F)

$$(F \times G)(\dots args \dots) \triangleq \left\{ \begin{array}{ll} F(\dots args \dots) & \text{iff } G(\dots args \dots) \\ 0.0 & \text{iff } \neg G(\dots args \dots) \end{array} \right\} \text{ intersection, analogous to } \cap$$

Algorithm X:

MDD *LRefine*($\mathbb{N}$ $\mathcal{N}_{transition\_labels}$, EV$^+$MDD $\mathcal{Q}_{[]}$, MDD $\mathcal{E}$, MDD $\mathcal{S}$) is
  local MDD $\mathcal{T}_{[]}$, MDD $\overline{\Delta\mathcal{E}}$, MDD $\mathcal{E}'$,
  1 $\overline{\Delta\mathcal{E}} \leftarrow \emptyset$
  2 for $t \in [0, \mathcal{N}_{transition\_labels})$ loop
  3 $\mathcal{T}_t \leftarrow proj_{\Sigma 3}((DC_2(\mathcal{Q}_t, \mathcal{S})) \times (DC_1(\mathcal{E}, \mathcal{S})))$ • $\mathcal{T}_t(a,b) = \Sigma c : (\mathcal{Q}(a,c) \times \mathcal{E}(b,c))$
  4 $\overline{\Delta\mathcal{E}} \leftarrow \overline{\Delta\mathcal{E}} \cup proj_{\vee 3}(DC_2(\mathcal{T}_t, \mathcal{S}) \uplus DC_1(\mathcal{T}_t, \mathcal{S}))$ • $\Delta\mathcal{E}(a,b) = \bigwedge t \in [0,t] : \bigwedge c : (\mathcal{T}_t(a,c) = \mathcal{T}_t(b,c))$
  5 end loop
  6 $\mathcal{E}' = \mathcal{E} \setminus \overline{\Delta\mathcal{E}}$ • $\mathcal{E}' = \mathcal{E} \cap \Delta\mathcal{E}$
  7 return $\mathcal{E}'$

```
MDD LumpingRefineClosure( ℕ 𝒩_transition_labels, EV+MDD 𝒬_[], MDD 𝒮, ℕ 𝒩_state_labels, MDD 𝒮ℒ_[] ) is
  local MDD ℰ_0, MDD ℰ, MDD ℰ_old,
   1 ℰ_0 ← ∅                                                  • Construct initial partition ℰ_0
   2 for l ∈ [0,𝒩_state_labels) loop
   3   ℰ_0 ← ℰ_0 ∪ DC_2(𝒮ℒ_l, 𝒮ℒ_l)
   4 end loop
   5 ℰ ← ℰ_0                                                  • ℰ(a,b) = ∃l ∈ [0,𝒩_state_labels) : (a ∈ 𝒮ℒ_l ∧ b ∈ 𝒮ℒ_l)
   6 repeat                                                   • ℰ ← LRefine( ℰ ) until ℰ = LRefine( ℰ )
   7   ℰ_old ← ℰ
   8   ℰ ← LRefine( 𝒩_transition_labels, 𝒬_[], ℰ, 𝒮 )
   9 until ℰ = ℰ_old
  10 return ℰ                                                 • E_{n_max}
```

Algorithm X, Closure of partition refinement (Markov lumping)

13 Acknowledgements

I thank my advisor for sharing his ideas and research.

Thanks to Min Wan for the use of the fork-join model and help with learning the SMART2 MDD library interface.

I thank the Lord for bringing me to the right advisor at the right time.

References

[1] Amar Bouali and Robert De Simone. Symbolic bisimulation minimisation. In *In Computer Aided Verification*, pages 96–108. Springer-Verlag, 1992.

[2] Randy E. Bryant. Graph-based algorithms for boolean function manipulation. *IEEE Transactions on Computers*, 35(8):677–691, August 1986.

[3] Gianfranco Ciardo and Radu Siminiceanu. Using edge-valued decision diagrams for symbolic generation of shortest paths. In Mark D. Aagaard and John W. O'Leary, editors, *Proc. Fourth International Conference on Formal Methods in Computer-Aided Design (FMCAD)*, LNCS 2517, pages 256–273, Portland, OR, USA, November 2002. Springer-Verlag.

[4] S. Derisavi. A symbolic algorithm for optimal Markov chain lumping. In O. Grumberg and M. Huth, editors, *Proc. 13th International Conference on Tools and Algorithms for the Construction and Analysis of Systems (TACAS'07)*, volume 4424 of *LNCS*, pages 139–154. Springer, 2007.

[5] Salem Derisavi. Signature-based symbolic algorithm for optimal markov chain lumping. In *Proc. Quantitative Evaluation of Systems (QEST)*, pages 141–150, 2007.

[6] Salem Derisavi, Holger Hermanns, and William H. Sanders. Optimal state-space lumping in markov chains. *Inf. Process. Lett.*, 87(6):309–315, 2003.

[7] Salem Derisavi, Peter Kemper, and William H. Sanders. Lumping matrix diagram representations of markov models. In *Proc. Int. Conf. on Dependable Systems and Networks (DSN)*, pages 742–751, Los Alamitos, CA, USA, 2005. IEEE Computer Society.

[8] Agostino Dovier, Carla Piazza, and Alberto Policriti. An efficient algorithm for computing bisimulation equivalence. theoretical computer science. *Theor. Comput. Sci*, 311:1–3, 2004.

[9] M. Fujita, P. C. McGeer, , and J. C.-Y. Yang. Multi-terminal binary decision diagrams: an efficient data structure for matrix representation. *Formal Methods in System Design*, 10:149–169, 1997.

[10] Holger Hermanns and Markus Siegle. Bisimulation algorithms for stochastic process algebras and their bdd-based implementation. In *ARTS '99: Proceedings of the 5th International AMAST Workshop on Formal Methods for Real-Time and Probabilistic Systems*, pages 244–264, London, UK, 1999. Springer-Verlag.

[11] Timothy Kam, Tiziano Villa, Robert K. Brayton, and Alberto Sangiovanni-Vincentelli. Multi-valued decision diagrams: theory and applications. *Multiple-Valued Logic*, 4(1–2):9–62, 1998.

[12] Y.-T. Lai and S. Sastry. Edge-valued binary decision diagrams for multi-level hierarchical verification. In *Proceedings of the 29th Conference on Design Automation*, pages 608–613, Los Alamitos, CA, USA, June 1992. IEEE Computer Society Press.

[13] Faron Moller and Scott A. Smolka. On the computational complexity of bisimulation, redux. In *Principles of Computing and Knowledge: Paris C. Kanellakis Memorial Workshop*, pages 55–59, San Diego, CA, USA, June 2003.

[14] Robert Paige and Robert E. Tarjan. Three partition refinement algorithms. *SIAM J. Comput.*, 6(16), December 1987.

[15] Scott Sanner and David McAllester. Affine algebraic decision diagrams (AADDs) and their application to structured probabilistic inference. In *Proc. IJCAI*, 2005.

[16] F. Somenzi. CUDD: CU Decision Diagram Package, Release 2.3.1. http://vlsi.colorado.edu/~fabio/CUDD/cuddIntro.html.

[17] Paul Tafertshofer, Lehrstuhl Fur Rechnergestutztes Entwerfen, Prof Dr. ing, K. Antreich, Prof. Dr. Massoud Pedram, Betreuer Ulf Schlichtmann, and Bernd Wurth. Factored edge-valued binary decision diagrams. In *Formal Methods in System Design*, pages 109–132. Kluwer, 1997.

[18] Min Wan, Gianfranco Ciardo, and Andrew S. Miner. Decision-diagram-based approximate steady-state analysis of large structured markov models. [in progress].

[19] Ralf Wimmer, Marc Herbstritt, and Bernd Becker. Forwarding, splitting, and block ordering to optimize bdd-based bisimulation computation.